# Assessing aboveground carbon stocks and forest structure metrics in the Mouila Oil Palm Concession Lot 2, Gabon

by

Mark Burton

Dr. John Poulsen, Advisor

May 2014

Masters project submitted in partial fulfillment of the

requirements for the Master of Environmental Management degree in

the Nicholas School of the Environment of

Duke University

2014

## Abstract

Growing demand for oil palm is driving its rapid expansion into the African tropics. While palm agriculture can be profitable, the conversion of tropical forests to oil palm monocultures tends to induce environmental degradation, loss of biodiversity, and significant carbon emissions. In this study, we evaluate the potential loss of biomass and the carbon emissions from conversion of a previously logged Gabonese forest to an oil palm plantation. We use a combination of field and LiDAR (Light Detection and Ranging) data to quantify and spatially model aboveground biomass (AGB), carbon stocks, and forest structure in the Mouila Lot 2 (ML2) oil palm concession in the Ngounié Province of Gabon. We established 30 1-ha plots using a stratified, random design. Mean AGB was 257.3 ± 73.8 and 345.8 ± 114.0 Mg $ha^{-1}$ for 20 plains and 10 plateau plots. Using a multiple linear regression model calibrated with field measurements to predict the spatial distribution of AGB from LiDAR metrics, we estimate the plains forest contain 4.15 Tg AGB (2.07 Tg C) and the plateau forests to contain 4.48 Tg AGB (2.24 Tg C). Using a conservative estimate of biomass saturation in oil palm monocultures (100 Mg $ha^{-1}$), we estimate that 1.19 Tg C would be emitted from conversion of the plains forest. The carbon density of these forests, even after selective logging, thus exceeds limits proposed by the Roundtable on Sustainable Palm Oil (RSPO). Due to the economic viability of oil palm agriculture and concessions already granted, oil palm development is not likely to stop in Central Africa. Creating regional standards for carbon emissions will allow the balancing of economic development and environmental objectives, while maintaining the framework of economic incentives for socially and environmentally responsible development.

# Table of Contents

# 1. Introduction

## *1.1. Oil Palm*

Industrial oil palm agriculture produces more than 34% of the world's vegetable oil and is a rapidly expanding sector in many developing economies (RSPO 2013). Palm oil derivatives are widely used for cooking oil, for biofuel production, and as a component of many processed foods and consumer items (e.g., cosmetics). It is estimated that palm oil can be found in one in ten supermarket products (Nellemann et al. 2007). Most of the approximately 14.6 million hectares (ha) of land are under palm cultivation are found in Asia (FAO 2009), although the crop is expanding in the Neotropics and Central Africa (Amigun et al. 2011).

Approximately 59% of the total carbon in the world's forests is sequestered in tropical forests (Dixon et al. 1994). Therefore conversion of tropical forests to oil palm plantations directly perturbs carbon cycling (Danielsen et al. 2009). Emissions caused by deforestation and land-use change, particularly in carbon-rich tropical forests, are one of the largest sources of anthropocentric carbon inputs into the atmosphere, accounting for as much as 20% of the total greenhouse gas emissions each year (Harris et al. 2012; Newell and Vos 2012; Venter and Koh 2012). Land-use change from 1990 to 2005 resulted in emissions of 1.5 ± 0.7 Pg C annually, most coming from deforestation and degradation of tropical moist forests (Le Quéré et al. 2009). Conversely, maintaining standing forest actively sequesters carbon from the atmosphere (Lewis et al. 2009; Gonzalez et al. 2010).

Tropical Africa alone is estimated to lose 5.2 million ha of tropical forest per year (Ramankutty et al. 2007), and the expansion of agriculture in the region will continue to drive this trend. Conversion of intact forests accounts for 55% of new agricultural land in the tropics,

while conversion of degraded forests accounts for a further 28% (Gibbs et al. 2010). As a result, the emissions from oil palm agriculture will be largely dictated by the status of the forest being converted, with lower biomass levels correlated with more degraded forests (Morel et al. 2011; Carlson et al. 2013). However, the magnitude of the net impacts of oil palm plantations on carbon emissions are uncertain, particularly in relatively under-researched regions like Central Africa, highlighting the need for additional research in this field (Koh et al. 2011; Paoli et al. 2011).

### *1.2. Impacts of oil palm development*

Oil palm growth is optimized in climatic conditions conducive for moist tropical forests, the most biologically rich terrestrial ecosystem. Therefore, the expansion of oil palm into these moist tropical forests can cause high biodiversity loss, particularly at the local scale (Sheil et al. 2009; Fargione et al. 2008; Meijaard and Sheil 2013). Gabon has 210 species classified as critically endangered, endangered and vulnerable on the IUCN Redlist (IUCN 2013). In addition, Gabon hosts great ape and elephant populations along with as many as 508 endemic vascular plants that will come under risk in palm oil concessions (The Forests of the Congo Basin 2010)

Land-use conversion of forest to oil palm monoculture by definition will alter forest structure and dynamics. However, the impacts of conversion penetrate into the remnant stands of forest. Fragmentation of forests increases the edge to core ratio of remaining forest patches; which, in tropical forests, increases temperature and decreases moisture compared to the interior (Murcia 1995; Laurance et al. 2002). Trees at forest edges are more vulnerable to being uprooted by wind events, progressively pushing the edge inward, further shrinking core habitat area (Saunders et al. 1991; Laurance et al. 2002). Land-use change, and subsequent road construction,

is typically correlated with an increase in human presence in the forest and is inevitably followed by hunting and further deforestation (Laporte et al. 2007; Poulsen et al. 2011). Chronic disturbance associated with resource extraction and with proximity to roads and villages has been shown to significantly alter many aspects of forest structure and function, maintaining characteristics similar to early successional environments (Horne and Hickey 1991; Kariuki et al. 2006; Souza et al. 2012).

Landscapes subject to oil palm development are characterized by fragmented remnant patches of natural forest. Rather than serving as hotspots of diversity, these patches tend to take on the attributes of the plantation with bird diversity in forest fragments resembling diversity within the actual oil palm plantation and not that of the original contiguous forest (Edwards et al. 2010).

In Southeast Asia, conversion of forest to oil palm plantations resulted in the loss of larger-bodied organisms at higher trophic levels across multiple taxa (Senior et al. 2012) and declines in bird species richness (Aratrakorn 2006; Koh and Wilcove 2008). In addition, land-use conversion, primarily to oil palm monocultures, in Sumatra, Indonesia is one of the primary drivers of orangutan habitat loss (van Schaik et al. 2001; Robertson and van Schaik 2001). It is estimated that 19% of the orangutan distribution in Borneo overlaps with undeveloped industrial oil palm concessions, suggesting that orangutan populations face continued population declines in these areas (Wich et al. 2012). In addition, orangutans are under increasing threat from conflict with humans. Concessions (e.g., oil palm, timber, etc.) increase human access to forests and thus increase the threat (Meijaard et al. 2011). Similarly, Central Africa is home to multiple species of great ape already threatened by habitat loss and human conflict (Walsh et al. 2003). The continued rapid expansion of the industrial oil palm sector could further threaten these

species without expanded efforts to mitigate the impacts of conversion to oil palm monocultures (IUCN 2013).

Altering three-dimensional forest structure has detrimental impacts on native fauna as well as the flora (Asner et al. 2008). The horizontal and vertical profiles of canopies influence the distribution of species, particularly bird species, due to habitat partitioning (e.g., MacArthur and MacArthur 1961; Erdelen 1984; Carey et al. 1991). An altered structure changes the distribution of forest resources and therefore impacts the interaction of species with their environment; a fact that holds true across a range of taxa, including mammals and insects as well as birds (Asner et al. 2008). All of these factors contribute to the loss of plants and animals from forests in a landscape matrix including oil palm monocultures.

### *1.3. Forest structure and spatial carbon stock modeling*

The ability to quantify biomass and other forest structure metrics (e.g., canopy surface height, basal area, stem density, etc.) will be a major step towards reliable implementation of sustainability and responsible development programs (e.g., Roundtable of Sustainable Palm Oil, RSPO) as well as carbon offset programs (e.g., Reducing Emissions from Deforestation and Forest Degradation, UN-REDD+). Further understanding the spatial and temporal distribution of these metrics will aid in the development of solutions for curbing global change as well as potentially understanding how changing landscapes are affecting native species, including threatened and endemic species.

The remoteness and lack of infrastructure in many tropical regions, including Central Africa, make fieldwork time-consuming and expensive. These obstacles mean historically relatively little work was done in the Congo Basin, even on small-scales. Regional and landscape

level studies are even more rare due to the difficulties and constraints in these regions. However, the pace of research on AGB in Central Africa has recently begun to accelerate with increased understanding of the importance of tropical moist forests in carbon cycling (e.g., Medjibe et al. 2011; Lewis et al. 2013; Ngomanda et al. 2014). The accurate quantification of forest metrics predicting landscape-scale patterns in carbon stocks can aid successful implementation of applicable best management practices for oil palm plantation establishment as well as for carbon sequestration programs.

Satellite remote sensing offers the practical ability to examine large regions at a broad-scale, but often at the expense of resolution. As a result, it provides little information on the heterogeneity of forests at the scale of plantation development. On the other hand, field measurements provide accurate, high-resolution data on a localized scale, but often do not account for potential landscape-scale heterogeneity and gradients. However, airborne LiDAR (Light Detection and Ranging), after calibration using systematic field inventories, can potentially bridge this gap as a tool for extrapolating field measurement data across landscapes while accounting for landscape heterogeneity (Asner et al. 2010). In addition to its high spatial resolution, it offers information on metrics difficult to assess in the field, such as vertical canopy profiles. Understanding the use of LiDAR metrics for characterizing levels of forest degradation and carbon accounting in the Congo Basin could provide insight into its utility as an instrument for landscape-scale monitoring and assessment for adaptive management in conservation planning and prioritization.

### *1.4. Palm oil expansion in Gabon*

Despite environmental impacts, oil palm development on deforested or degraded land can

be economically feasible (Fairhurst and McLaughlin 2009). In some country-dependent contexts, it is considered a sustainable option accounting for multiple goals of socially and environmentally responsible economic development (Daily 1995, Koh et al. 2009). The European Biofuels Directive of 2003 created an enhanced market for biofuels to encourage European countries to achieve goals for replacing fossil fuels with biofuels. As the most productive biofuel source, Central African oil palm markets thus expanded because of their close proximity to the burgeoning biofuels market (Nellemann et al. 2007; Fargione et al. 2008). As a result, conversion of forested land to oil palm plantations is one of the more economically profitable land uses (Wilcove and Koh 2010). Counterproductively, the majority of oil palm development is occurring on carbon-rich forested land, so European efforts to reduce carbon emissions from fossil fuel combustion by the transportation sector is actually driving up carbon emissions due to deforestation (Nellemann et al. 2007). Greater efforts need to be made to understand the impacts of oil palm development, both on carbon cycling and biodiversity, to mitigate these impacts while realizing the economic benefits of development in the tropics.

RSPO developed standards and best practices for planning and management that minimize the social and environmental impacts of oil palm development, including on both biodiversity and carbon stocks. Consumers pay a premium price, estimated at 8 to 15% higher than the traditional product, for RSPO certified oil from plantations that meet these criteria (Wilcove and Koh 2010; RSPO 2013). For example, the RSPO mandates buffer zones around watercourses, restricts the use of pesticides, and requires implementation of a program for transparent communication with communities surrounding plantations, among many others. The RSPO has also considered various options for limiting carbon emissions from deforestation, including possibly prohibiting agriculture in forest that would have net carbon emissions from

land-use conversion (RSPO 2011). In Southeast Asia, the aboveground biomass (AGB) of oil palm plantations saturates at approximately 100 Mg $ha^{-1}$ (Morel et al. 2011). This would serve as a *de facto* threshold with carbon emissions disqualifying plantations with higher pre-conversion biomass levels from RSPO certification. Many of these criteria, however, were developed for the leading producers of oil palm in Southeast Asia. It is unclear to what extent these standards apply to the Congo Basin.

The Government of Gabon seeks to become a leading exporter of oil palm by 2020 in an effort to expand and diversify its economy (2nd Palm Oil Africa 2013). Gabon is believed to have over five million ha of suitable land for palm agriculture and aims to expand production by 400% to 250,000 tons per year (2nd Palm Oil Africa 2013). Gabon is ideally situated to supply both the Central African and European markets with much lower shipping costs compared to Southeast Asian producers. The Government of Gabon has offered a series of economic incentives to companies to encourage the development of oil palm plantations, including holding a 30% stake in some oil palm developments. This 70:30 split includes a deal with Olam Palm Gabon for the first phase of oil palm development, a reported 300 million dollar total investment for over 50,000 ha planned to meet RSPO criteria (Versi 2012).

For Gabon to meet both its development and conservation goals, it is necessary to evaluate the likely environmental impacts of palm agriculture so that appropriate management regulations can be developed. While international standards, such as RSPO, can help guide the process, it is important to assess whether they can be realistically implemented in Central African forests. In this study we aim to (*i*) quantify AGB and carbon stocks for Lot 2 of the Mouila concession (ML2) using the RAINFOR plot inventory methodology, in order to estimate the carbon emissions likely to occur with deforestation of a degraded Gabonese forest for palm

agriculture. In addition, (*ii*) the AGB and carbon stocks in plains and plateau forests are compared as a means of evaluating whether setting aside the proposed high conservation value forest (HCVF) on the plateau would conserve important carbon stocks. This study also (*iii*) models the spatial distribution of carbon stocks across ML2 based on forest structure metrics derived from a LiDAR dataset. Lastly, (*iv*) we compare the results from the RAINFOR plot inventory methodology and a rapid inventory methodology to assess the accuracy of the faster approach to AGB inventory.

# 2. Methods

### *2.1. Study Region*

In 2011 and 2012, the Government of Gabon leased the 67,000 ha Mouila concession in the Ngounié Province to Olam Gabon for oil palm production. Olam is a multinational agro-business based in Singapore. It supplies industrial raw materials and food, including cocoa, coffee, cashews, rice, and cotton, and operates at multiple levels of the supply chain for these products (Olam 2014). Olam is one the largest investors in Africa outside the oil and gas industry, and has committed to invest up to 2.5 billion USD in Gabon starting in 2012, with an initial focus on oil palm, rubber, fertilizer production, and development of the Nkok Special Economic Zone (Versi 2012).

The Mouila concession is divided into two lots: Mouila Lot 1 (ML1; 35,300 ha) and Mouila Lot 2 (ML2; 31,800 ha). Whereas palm agriculture was initiated in ML1 in early 2013, ML2 is at the conversion stage, with forest clearance scheduled to commence in May 2014. ML2 is believed to be old timber concession that was selectively logged, with more intense extraction

occurring on the plains compared to the plateau, primarily for reasons of accessibility (Ecosphere 2013; Summary Report 2013). Observations of skidder trails and cut stumps in the concession confirm its status as a timber concession (Appendix E). It is located along the road corridor, which is characterized by widespread anthropogenic conversion of forest to savannah and resource extraction, connecting the towns of Mouila and Mandji (Figure 1). Lot 2 (01°42'S, 10°25'E) consists of lowland mixed tropical moist forest. The mean monthly precipitation ranges from 4 to 382 mm for a total of approximately 2000 mm $yr^{-1}$; exhibiting a long dry season from June through September (Figure 2; Hijmans et al. 2005). The mean temperature ranges from 23 to 26°C with an annual mean temperature of 25.7°C (Hijmans et al. 2005). ML2 can be separated into two broad forest types: (1) a plateau that will likely be designated as high (HCVF) set-aside; and (2) a relatively flat plains that will be developed for oil palm agriculture (Figure 3).

### *2.2. Field Measurements*

#### *2.2.1. Study Design*

Between August and November 2013, the Gabon National Park Agency's (ANPN) forest monitoring team inventoried 30 1-ha plots (40 x 250 m) in ML2. The ANPN team is trained in standard RAINFOR protocols for plot establishment and measurement (Phillips et al. 2009), and established over 100 plots as part of the country's national forest monitoring system. Within ML2, we determined the location of the plots using a stratified-random design to ensure a wide spatial distribution of plots and an unbiased selection of forest. We superimposed a grid of cells over the concession for each of the strata (plateau and plains), randomly placing two points within each cell. To directly compare our results with Ecosphere's results, whenever one of our

grid cells encapsulated Ecosphere plots, we selected the Ecosphere plot nearest our random point for our survey. We established 10 plots on the plateau and 20 plots in the plains (Figure 4). Whereas the plains plots will likely be deforested for palm oil agriculture, the plateau plots were established as permanent plots to monitor forest dynamics over time. Eighteen of the 30 plots had been previously surveyed by Ecosphere.

The field teams inventoried, mapped and measured each individual tree with a diameter-at-breast height (DBH) ≥ 10 cm. DBH was measured at a height of 1.3 m from the ground, except when trees had stilt or buttress roots or the stems were not cylindrical at that height. Samples from individuals that could not be identified in the field were collected for herbarium identification in Libreville, Gabon. In addition, individuals were assessed for general status and presence of lianas. Field teams measured tree height using a laser hypsometer, taking heights of 10 randomly selected trees from each of 5 DBH subclasses (10-20 cm, 21-30 cm, 31-40 cm, 41-50 cm, and >50cm).

*2.2.2. Aboveground Biomass*

We built a series of regression models (linear, quadratic, and polynomial) for each plot to estimate the relationship between tree height and the natural log of tree diameter from the data. We examined the residuals from each model to evaluate model fit to the data, and compared models to maximize adjusted $R^2$. The best model was then used to predict tree heights from the associated DBH of each individual stem.

Diameter ($D$) measurements were converted to AGB and carbon stocks using published allometric equations for moist forests that also include terms for wood density ($\rho$) and tree height ($H$; Chave et al. 2005, Ngomanda et al. 2014).

Chave Moist Forest (CMF):

$$AGB = \rho \times \exp(-1.499 + 2.148 \times \ln(D) + 0.207 \times -0.0281 \times ln(D)^3)$$

Chave Moist Forest with Height (CMFH):

$$AGB = \exp(-2.977 + \ln(\rho \times D^2 \times H))$$

Ngomanda Moist Forest (NMF):

$$AGB = \exp\left(-4.0596 + 4.0624 \times \ln(D) - 0.228 \times ln(D)^2 + 1.4307 \times ln(\rho)\right)$$

Ngomanda Moist Forest with Height (NMFH):

$$AGB = \exp\left(-42.5680 + 0.9517 \times \ln(D^2 \times H) + 1.1891 \times \ ln(\rho)\right)$$

We used published species-specific wood density values when available (Zanne et al. 2009). In the absence of species, genus, or family wood density values, we substituted the mean wood density for the plot. The AGB for each plot was calculated by summing all the trees within a plot. AGB was assumed to be 50% carbon (Chave et al. 2005).

The Chave et al. (2005) allometric equations are derived from a comprehensive database of 2,410 trees with a diameter greater than 5 cm from America, Asia, and Oceania. The geographical range of the represented tropical forests makes them robust and widely applicable. As a result, these equations have been used in a large number of studies and are useful for comparison. Chave et al. (2005) is the most widely reported allometric equation in Africa (Ngomanda et al. 2014). The inclusion of a height variable in the equation reduced error estimates from 19.5% to 12.5%, so including height measurements is recommended when possible (Chave et al. 2005). A drawback of the Chave et al. (2005) equations is that they do not include data from Africa. Ngomanda et al. (2014) constructed an allometric equation using 101 trees from 10 species representing a range of wood densities. By applying the CMF equation to the trees in their study, Ngomanda et al. (2014) found that it systematically overestimated biomass. However, Ngomanda et al.'s allometric equations are based on a much smaller sample size and few species in a localized region in northeastern Gabon. Our study includes trees from

55 families, so we employ Chave's more generalized equations. In addition, Ecosphere used the CMF equation in their biomass estimates for ML2, so we also use this equation to directly compare our results with their biomass estimates.

### *2.3. LiDAR Metrics*

LiDAR techniques have been used to spatially map three-dimensional structure of forests (Lefsky et al. 2002; Lim et al. 2003). Raw LiDAR is a three-dimensional cloud of points derived from the length of time a laser pulses travels from emission until returning to the sensor, which can be analyzed to allow inferences on the physical dimensions of trees or stand level metrics (Lefsky et al. 2002; Coops et al. 2007). The raw LiDAR data are processed to separate ground returns from vegetation, producing information on canopy height, tree density, and horizontal and vertical canopy structure. By combining LiDAR data with field inventory data through modeling, the forest structure data can be converted to spatial estimates of forest biomass and carbon with high accuracy (Gonzalez et al. 2010; Jubanski et al. 2013). Past studies demonstrated high correlations between LiDAR metrics and the AGB and carbon density from forest field measurements (e.g., Drake et al. 2002; Lefsky et al. 2005; Gonzalez et al. 2010; Meyer et al. 2013).

Olam commissioned the Moroccan company, SEPRET, to conduct aerial LiDAR collection over the Mouila concession in September 2011. A Leica ALS 60 sensor mounted on a Cessna 402 airplane flew at an altitude of 1,500 feet and at an average speed of 120 Ktas. The pulse and scan frequencies were 96.1 KHZ. The dataset was discrete, small-footprint, with between one and four returns recorded for each pulse and between five and 20 returns per $m^2$. SEPRET also produced a 2-$m^2$ resolution digital terrain model (DTM) using a propriety

algorithm to separate ground points from vegetation returns. The raw LiDAR *.las* files provided by Olam were read into *ArcGIS 10.2* software (ESRI 2013). The (x,y,z) coordinates of each LiDAR return as well as other attributes (e.g., intensity) were then extracted.

The first LiDAR return is assumed to be the canopy surface in a forested area. A roving window moved across the landscape calculating the mean *Z* value to create a continuous 2-$m^2$ resolution surface. The DTM values were subtracted from the canopy surface to create a canopy height model for ML2. The mean values were also calculated for $2^{nd}$, $3^{rd}$, and $4^{th}$, and all returns to create height models using the same process. We then separated the understory, midlevel, and canopy based on the percentile methodologies in Lesak et al. (2011).

### *2.4. Biomass Model*

Ordinary least squares multiple linear regression was used to model the relationship between the LiDAR metrics and AGB from field measurements The LiDAR metrics derived for analysis included mean, standard deviation, maximum, minimum, range, and $10^{th}$, $25^{th}$, $50^{th}$, $75^{th}$, $90^{th}$ percentiles of heights derived from the $1^{st}$, $2^{nd}$, $3^{rd}$, $4^{th}$, and all LiDAR returns (Appendix B). Two regression models were created to predict AGB from the LiDAR metric explanatory variables; one with CMF and one with CMFH as the dependent variable. The LiDAR-derived metrics that were significantly correlated (Pearson's product-moment, $\alpha = 0.05$) with AGB from field measurements were included. The correlations between LiDAR metric explanatory variables were then screened for Pearson's product-moments exceeding 0.7 to account for multicollinearity. The variable in the pair more highly correlated with the AGB value was kept and the less correlated variable was eliminated from the model. The remaining variables served as the input predictor variables in a multiple linear regression model. A nested approach was

employed to remove these predictor variables. For each progressive iteration, the predictor variable with the least significant explanatory power was removed from the model. The model was then tested against the previous model using an ANOVA on a $\chi^2$ distribution. This process was iterated until removing the variable caused a significant loss of explanatory power in order to identify the most parsimonious model.

These models were then applied to predict the spatially explicit carbon densities for the entirety of ML2. The predictor variables in the final model were calculated for each individual 2-$m^2$ using a geographically centered 1 ha (40 x 250 m, N-S orientation) focal area, consistent with field measurements methodology for deriving plot-based metrics.

### *2.5. Comparison of Ecosphere Aboveground Biomass Values*

As part of the environmental impact assessment of ML2, Ecosphere, an independent Gabonese environmental consulting company, installed 52 plots with a systematic equidistant grid design, and then used a rapid inventory methodology to characterize the forest and estimate forest biomass in ML2 (Ecosphere 2013). Ecosphere used 1-ha plots (40 x 250 m), measured the diameter of each tree stem ≥ 10 cm DBH, and identified each stem to species.

### *2.6. Statistical Analyses*

We compared plot biomass, tree diameter, tree height, basal area, and wood density between the plateau and plains forests. We also evaluated AGB differences between our inventory and the concurrent inventory conducted by Ecosphere. In all cases, we assessed the normality of the data and then used the appropriate parametric or non-parametric test for these

comparisons. All statistical analyses were conducted with the R-statistical package (R-Core Team 2013). All geospatial data were projected in WGS 1984 UTM Zone 32S.

# 3. Results

### *3.1. Field Measurements*

In total, we measured and mapped 12,821 individual trees from 55 families in the 30 1-ha plots. Euphorbiaceae, Burseraceae, Olacaceae, and Annonaceae were the most represented families on the plateau; whereas Olacaceae, Ebenaceae, Caesalpiniaceae, and Euphorbiaceae were the most represented families on the plains. 70.7% of the stems were identified to species, and 88.6% of the stems were identified to the genus level. Two of the plains plots were located at the transitional zone between forest and savanna, with more than one third of their areas lacking stems ≥ 10 cm diameter. We removed these plots from our comparison of plains and plateau forests as our focus was on forest structure, not variation between different habitat types.

The distribution of tree diameters differed significantly between the plains and plateau forest plots. Small diameter individuals (< 30 cm) were the most abundant at both sites; however, the plains had a more pronounced inverted J-curve with a higher proportion of small diameter trees than the plateau plots (Kolmogorov-Smirnov test: $D = 0.026$, $p = 0.027$; Table 1; Figure 5). Plateau plots contained significantly higher numbers of stems than plains plots (498.7 stems $ha^{-1}$ compared to 421.6 stems $ha^{-1}$; Table 1; Figure 6, Appendix D) In addition, the basal area of plateau plots was 5.5 $m^2$ $ha^{-1}$ higher on average than plains plots (Table 1; Figure 6). Plot-scale mean per tree height and basal areas did not differ between the two sites (Table 1; Figure 6).

There was also no significant difference when the mean wood density was compared between plains and plateau plots ($t_{27} = 1.702$, $p = 0.100$; Table 1).

A comparison of the AGB allometric equations were conducted to assess differences (Figure 7). Regression analysis for each equation of AGB as a function of diameter indicates the difference between the AGB per tree calculated without and with a height variable increases with increasing diameter for both the Chave et al. and Ngomanda et al. pairs of equations. With every 1% increase in diameter, the AGB per tree is expected to increase by 2.54% and 2.44% for CMF and CMFH, respectively ($ln$(CMF) = -8.93 + 2.54($ln$(diameter), $F_{1,12819} = 452800$, $R^2 = 0.973$, $p < 0.001$; $ln$(CMFH) = -8.74 + 2.44($ln$(diameter), $F_{1,12819} = 203800$, $R^2 = 0.941$, $p < 0.001$). Similarly, every 1% increase in diameter results in 2.54% and 2.31% for NMF and NMFH, respectively ($ln$(NMF) = -9.13 + 2.54($ln$(diameter), $F_{1,12819} = 210000$, $R^2 = 0.943$, $p < 0.001$; $ln$(NMFH) = -8.45 + 2.31($ln$(diameter), $F_{1,12819} = 164000$, $R^2 = 0.928$, p < 0.001). These comparisons show that including the height variable increasingly reduced the AGB per tree estimate relative to the estimate excluding height as diameter increased.

Using Chave et al.'s allometric equation for moist forest and incorporating tree heights (CMFH), we estimated AGB to range from 108.9 to 501.5 Mg ha$^{-1}$ (Appendix A). The average biomass across ML2 was 288.9 ± 98.9 Mg ha$^{-1}$ (95% CI = [250.9, 327.0]), with a mean biomass of 257.3 ± 73.8 (95% CI = [220.6, 294.0]) and 345.8 ± 114.0 Mg ha$^{-1}$ (95% CI = [264.2, 427.4]) for plains and plateau plots, respectively. As a result of these differences, when height was incorporated in AGB metrics, plateau plots contained significantly higher biomass than plains plots (CMFH: $t_{13} = 2.21$, $p = 0.045$; NMFH: $t_{13} = 2.20$, $p = 0.046$; Table 1). However, the AGB of plains and plateau plots was not significantly different at the 0.05 significance level using

allometric equations that did not incorporate height (CMF: $t_{13} = 2.14$, $p = 0.052$; NMF: $t_{13} = 2.10$, $p = 0.055$; 95% CI = [-174.8, -2.2]; Table 1, Figure 8).

By multiplying the mean biomass by the forest area in the plains and plateau, we estimate an overall AGB for Mouila Lot 2 of 9.09 ± 2.82 Tg using the CMFH equation. This equates to approximately 4.55 ± 1.41 Tg C stored in the aboveground forests of Mouila Lot 2. The plains forests account for 4.21 ± 1.21 Tg AGB or 2.11 ± 0.61 Tg C. Assuming that a mature palm oil plantation can accumulate 100 Mg $ha^{-1}$ after 20 years, the future plantation area would be expected to hold 1.78 Tg of biomass (0.89 Tg C). Therefore, conversion of the plains area of ML2 will result in the net loss of 2.44 ± 1.21Mg $ha^{-1}$ of biomass or the net emission of 1.22 ± 0.61 Tg C from the aboveground vegetation alone.

### *3.2. LiDAR metrics*

Differences in the canopy heights were found between the plains and plateau areas based on the LiDAR analysis (Figure 9, 10). The plateau forest plots have significantly taller mean canopies (28.1 ± 6.58 m) than the plains plots (23.0 ± 3.21 m), even after removing plots 1 and 2 ($t_{11} = -2.294$, 95% CI = [-9.93, -0.229], $p = 0.0416$). These results differ from the field measurements, which found no difference between the mean stem height of plots in plains and plateau forests ($W = 73$, $p = 0.436$). The mean height derived from all LiDAR returns was a significant predictor of the maximum height of the canopy from field measurements. However, it only explained 22.7% of the observed variability in maximum field measurements, while other explanatory models fared worse ($R^2 = 0.227$, $F_{1,28} = 9.529$, $p = 0.005$).

There were also differences in the distributions of LiDAR returns when classified into three main categories (gaps, midlevel, and upper canopy) of forest structure. The gap returns

from plains and plateau plots were similarly very low at 2.62% and 2.96%, excluding plots 1 and 2. However, 76.9% of the plains forest was classified as midstory vegetation compared to 55.3% for plateau forest. Similarly, 20.4% of the plains forest was classified as upper canopy, while 41.7% of the plateau was categorized as upper canopy.

We constructed pseudo-wave canopy structure plots to visualize the difference in canopy density at increasing heights above the forest floor (Figure 11). With few exceptions, the profiles show a unimodal distribution indicating forests with thick canopies and few gaps. However, the pseudo-wave distributions reveal trends in the differences between the plateau and plains forest plots. Overall, the plateau plots appear to have both greater intra- and inter plot heterogeneity. Excluding plots 1 and 2, the variance was significantly higher in plateau forest than plains forest ($F_{17,9}$= 0.239, 95% CI = [0.182,1.925], $p < 0.011$). These results suggest plateau forests, in comparison to plains forests, had a more heterogeneous, diverse, and taller canopy height distribution.

These profiles also provided interesting insights into a subset of the plots. Plots 1 and 2 stood out due to the extremely low canopy heights with means of 8.49 and 8.63 meters and a median of 0.72 and 7.84 m. They show profiles characteristic of an early successional habitat. For example, plot 2 was dominated by grasses and shrubs, with a second peak of vegetation about 10 meters tall, likely fast-growing, shade intolerant species. This pattern is typical an open forest structure with a bimodal distribution of returns with a peak at a low canopy height and a second peak at ground level.

Although not as extreme, plot 23 also had relatively low canopy heights compared to the other plateau plots at 13.73 meters, an almost 12 meters shorter mean canopy height than any of the other plateau plots. Overall, the majority of the plots showed a relatively heterogeneous range

of heights in both location types, plateau and plains, with the plateau forests peaking at a slightly taller mean canopy surface height.

### *3.3. Biomass Models*

The mean height of all points derived from the LiDAR dataset proved to be a relatively good predictor of AGB, explaining 80% of the variability in the biomass (CMF = -36.199 + 16.277($Ht_{LiDAR}$); $R^2 = 0.798$; $F_{1, 28} = 112.9$, $p < 0.001$; Figure 12). A one-unit increase in LiDAR-derived canopy height results in a 16.22 Mg $ha^{-1}$ gain in AGB. The mean LiDAR-derived height explained less of the variation in AGB for CMFH (CMFH = -23.341 + 13.542($Ht_{LiDAR}$); $R^2 = 0.522$; $F_{1, 28} = 32.67$, $p < 0.001$; Figure 12). A one-unit increase in LiDAR-derived canopy height results in a 13.43 Mg $ha^{-1}$ gain in AGB.

The better CMF spatial model predicts that the plains contain 4.86 Tg AGB (excluding savannah area) and 2.43 Tg C, while the plateau forests contain 5.26 Tg AGB and 2.63 Tg C (Table 2; Figure 13). However, the CMFH model is more conservative and when combined with the saturation point on oil palm plantation, the CMFH model would predict conversion from tropical forest to plantation to release 1.19 Tg C (Figure 14).

The CMFH model consistently predicts lower carbon densities in comparison to the CFM model, except in savannah areas of ML2 (Figure 15). The difference between the two models is exacerbated in areas with higher canopy heights. This result is consistent with expectations given the positive correlation between stem diameter and height (Figure 16) and the increasing difference AGB per tree for CMF and CMFH seen with increasing diameter (Figure 7).

### *3.4. Comparison of Ecosphere Aboveground Biomass Values*

Ecosphere reported biomass estimates of 353.5 ± 168.9 Mg ha$^{-1}$ on the plains and 435.7 ± 155.7 Mg ha$^{-1}$ on the plateau using the CMF allometric equation for all 52 of their 1-ha plots (Ecosphere 2013). Their estimate of mean AGB for the plains was 14% higher and their estimate for the plateau forest was 12% higher than our CMF estimates. Chave et al. (2005) recommend using the CMFH allometric equation, which produces AGB estimates that are 17% (plains) and 11% (plateau) lower than our CMF results. Unfortunately, the rapid survey method did not include measurement of tree heights, resulting in relatively high estimates of biomass.

We directly compared our biomass estimates to Ecosphere's estimates for the 18 corresponding field plots using the CMF equation. There was no significant difference between the biomass results produced by the two methods ($t_{17} = 0.809$, $p = 0.430$). Interestingly, comparison of AGB between only shared plots indicates that Ecosphere mean AGB estimates are 8% and 6% lower than the mean plains and plateau, respectively, plot estimates from our study. Conversely, the CMF results from Ecosphere were not a significantly correlated with the CMF results from this study at the 0.05 level. Estimates of AGB from Ecosphere varied from being 197.7 Mg ha$^{-1}$ higher to 309.3 Mg ha$^{-1}$ lower than our results (Appendix C).

## 4. Discussion

### *4.1. Estimation of aboveground biomass*

Based on field data, we calculated that on average Mouila Lot 2 holds 288.9 Mg ha$^{-1}$ AGB. By multiplying the mean AGB ha$^{-1}$ for the plains (257.3 Mg ha$^{-1}$ AGB) and plateau (345.8 Mg ha$^{-1}$ AGB) forests by their respective area, we estimate that ML2 holds 9.09 ± 2.82 Tg AGB and 4.55

± 1.41 Tg C. Our estimate of AGB per hectare is slightly higher than that estimated for Gabon on average. A preliminary analysis of 73 forest plots determined mean biomass to be 273.8 Mg $ha^{-1}$ (95% CI = [245.3, 301.2]), or an average carbon stock of 136.9 Mg $ha^{-1}$ (ANPN 2013). The estimate of mean biomass for Gabon, however, comes from forest plots located in all forest types, including secondary and swamp forest, and all land-uses across the country. The CMF AGB estimates for ML2 (338.0 ± 87.7Mg $ha^{-1}$) are also comparable to CMF estimates in other previously logged forests of the Congo Basin that range from 335 to 386 Mg $ha^{-1}$ (Medjibe et al. 2011; Medjibe et al. 2013; Poulsen et al. 2013).

### *4.2. LiDAR Metrics*

#### *4.2.1. Comparison of LiDAR derived metrics between plains and plateau forest*

The LiDAR canopy heights were significantly taller in plateau forest compared to plains forest. The spatial distribution and pattern of these vertical stratums is important for interactions with the flora and fauna that use the ecosystem. The plateau had more LiDAR returns that were classified as upper canopy level in comparison to the plains, which saw a shift in more than 20% of these upper canopy returns to midstory and had a more homogenous canopy surface distribution. These trends are consistent with the perception that the plains forest was more intensively logged than the plateau forest. More heavily logged areas would be expected to have more homogenous canopy heights and fewer tall canopy trees, as was observed in the plains forests. As a result, the plateau area had a more complex three-dimensional forest structure. Although response to forest structure is highly complex and dependent on species, in some cases more complex canopy structures can support higher biodiversity levels. For example, community composition of ant species varies along the vertical strata of forests suggesting partitioning

similar to that observed in birds based on vertical canopy structure and heterogeneity (MacArthur and MacArthur 1961; Clawges et al. 2008; Neves et al. 2013;)

Interestingly, plot 23 had a much different forest structure than the other plateau plots and a lower mean canopy height. This can likely be explained by the presence of an old skidder trail bisecting the plot (Appendix E). The skidder trail is evidence of past logging activities within the concession and on accessible sections of the plateau. It also provides further evidence that logging intensity may be a driving force behind forest structure in ML2.

*4.2.2. LiDAR comparison with field measurements*

Interestingly, the LiDAR canopy height analysis showed significantly taller canopy height returns in plateau forest plots while the field measurements did not show a similar trend. LiDAR canopy heights only represent the upper surface of the canopy and do not provide information on individual stems. LiDAR height metrics are not necessarily meant to correspond to on-the-ground measurements of individual stems but rather can predict AGB and other secondary forest characteristics after calibration with plot level field measurements. The high density of LiDAR pulses (5-20 returns $m^2$) compared to the relatively much larger area of the horizontal crown structure of tropical species means that a single large crown will have many separate LiDAR returns input into the mean canopy height calculation. Thus LiDAR can over-represent taller stems with large canopies. On the other hand, heights measured in the field account for each stem only once and include shorter stems shaded by large crowns in plot-scale metrics. This disparity is seen in the fact that 22 of the 30 plots in this study had mean LiDAR-derived canopy heights that were taller than the corresponding mean height from field measurements. Five of the plots that did not exhibit this trend were also the five plots with the shortest mean canopies, with all these plots within the 12 shortest canopies. Shorter canopies decrease the likelihood of taller

stems having a disproportionate effect on height metrics and thus are likely to show consistent differences between LiDAR and field heights.

### *4.3. Biomass Models*

The spatial models derived from LiDAR data proved to have remarkably similar results as those derived from field measurements. The model predicted 5.06 Tg C compared to 5.3 ± 1.3 Tg C from field measurements using the CMF equation. Similarly, the CMFH model predicted 4.31 Tg C compared to 4.5 ± 1.4 Tg C from field measurements.

Subtracting the CMF from CMFH biomass models enables us to examine spatial patterns in the difference between estimated AGB across ML2 to better understand how the models perform. Consistent with expectations, there a strong spatial overlap of areas with taller canopy heights with larger differences between the two models. In this study, we found that with increasing diameter, the AGB per tree become increasingly divergent and increasing diameter is correlated with increasing stem height. The reduction of AGB in the model incorporating the height variable is consistent with previous results for logged forests. Morel et al. (2011) found that inclusion of height in allometric equations leads to lower estimates of AGB in logged forests, but leads to high estimates of AGB in unlogged forests.

The ability to reliably quantify and monitor forest biomass and carbon will be a major step towards implementation of sustainable development programs (e.g., RSPO standards) as well as carbon offset programs (e.g., REDD+). Accurate quantification of these metrics at a large scale, especially in the under-studied areas such as the Congo Basin, is currently an obstacle to successful implementation of best management practices for oil palm establishment as well as carbon payment options. LiDAR methodologies can distinguish, after calibration using

field inventories, areas of high biomass and thus can be a valuable methodology for prioritizing future conservation areas. In particular, remote sensing technologies allow biomass estimation over much greater areas than on-the-ground field measurements and can account for spatial heterogeneity that may be missed by field measurements alone.

Understanding the spatial patterns of these metrics is a tool to help curb global change by identifying areas with high carbon densities in order to improve conservation prioritization based of carbon emission mitigation. In order for these programs to be implemented, reliable methodologies must be in place in order to accurately quantify carbon stocks for greenhouse gas inventories. Temporal monitoring of these stocks for assessment and enforcement of credits for forest conservation and reforestation is a necessity. In addition, identifying spatial and temporal patterns in forest structure has the potential to offer insights into how changing landscapes are affecting native species, including threatened and endemic species. For example, chimpanzees select their sleeping platforms based on structural properties of available trees (Hernandez-Aguilar et al. 2013; Samson and Hunt 2014). Thus, understanding the use of LiDAR metrics for characterizing levels of forest degradation and carbon accounting in the Congo Basin could provide insight into its utility conservation and development planning and prioritization.

The AGB results from this study proved to be substantially higher than the biomass estimates derived from a pan-tropical spatial map created from satellite data augmented with LiDAR observations and field measurements (Baccini et al. 2008). Estimates from the Baccini map are 4.6 Tg AGB and 2.3 Tg carbon, compared to 8.6 Tg AGB and 4.3Tg C from the LiDAR-based CMFH calculations in this study. This difference between these estimates highlights that coarse resolution estimates from satellite remote sensing introduce a great deal of error at the local scale. For accurate estimates of biomass and carbon at the scale of a concession,

it is still necessary to collect *in situ* data to calibrate spatially explicit models. LiDAR provides an intermediate scale at very high spatial resolutions that can be used to extrapolate field measurements across landscapes at the scale of plantation development.

### *4.4. Comparison of Ecosphere Aboveground Biomass Values*

Although the direct, pairwise comparison of the AGB estimates from this study with those from a rapid inventory method employed by Ecosphere did not find a significant difference, it is likely an artifact of the high variability between the data. The Ecosphere results were neither consistently higher nor consistently lower than the results calculated in this study. A few explanations could explain the discrepancy. One possibility is that this is a true result and the two methodologies do not result in correlated AGB, thus indicating random chance is involved in the AGB difference between the two methodologies. It is also possible, and perhaps more likely, that there are discrepancies in the exact geographic location of plots. Ecosphere did not delineate plot boundaries and thus different stems may have been included compared to our study. In a previous study, large trees (> 70 cm diameter) accounted for less than 1% of stems but contributed over 14% of AGB (Clark et al. 2004). As a result, even a small offset in the plots location could strongly influence the estimated AGB in either direction. This possibility is reflected by our study measuring 8,294 stems while Ecosphere measured only 5,928 stems in the corresponding plots.

# 5. Conclusions

Development of oil palm in previously logged forests of the Mouila Lot 2 plains would result in the loss of 78.7 Mg C $ha^{-1}$ more than recommended by RSPO (using the CMFH equation for the plains). The total carbon emissions from aboveground vegetation would be approximately 1.2 Tg C after accounting for the future oil palm biomass. Even though the RSPO has not currently instituted a strict threshold for acceptable carbon loss in conversion of tropical forests to oil palm plantation, it seems unlikely that any secondary or degraded forest in Gabon would qualify given this finding. The final recommendations of the RSPO Greenhouse Gas Working Group 2 concluded that oil palm expansion should not result in net carbon emissions when balancing land-use conversion emissions with sequestration from one rotation of oil palm (RSPO 2011). The area of ML2 that could be converted to oil palm and result in no net carbon emission is limited almost exclusively to areas of savannah (Figure 17). Gabon is still 85% forested so it is likely that this RSPO standard would exclude Gabon from the sustainable palm agricultural sector, conflicting with the country's stated development goals.

Morel et al. (2011) found that severely degraded forests in Malaysian Borneo rarely exceeded 150 Mg $ha^{-1}$. Logged peat forests in Southeast Asia have been found to have biomass values of around 178 Mg $ha^{-1}$, with a similar value found in a logged Dipterocarp forest after an 18 year recovery period (Jubanski et al. 2013; Berry et al. 2010). Although these values are substantially lower than those found in ML2, they still exceed the biomass level at which oil palm saturates (100 Mg $ha^{-1}$) indicating these degraded forests would also lead to net carbon emissions. As a result, a strict standard may not prove feasible as over 80% of the world production is based in Southeast Asia (Koh and Wilcove 2007).

Southeast Asia has already experienced widespread development and growth; Malaysia alone has expanded their oil palm industry from 641,791 ha to over 5 million ha between 1975 and 2011 (Malaysia Palm Oil Board 2011). This scale of development has not been seen in Gabon or in other Central African countries. Over 85% of Gabon is covered by forest, and its gross deforestation rate was estimated at only 0.08% from 1990 to 2000 and declined to 0.07% from 2000 to 2005, in addition the net deforestation rate actually declined to 0.0% from 2000 to 2005 due to an increase in reforestation rate from 0.03 to 0.07% during the same time periods (The Forests of the Congo Basin 2010). However, the scale of these metrics would not be accounted for in the creation of global RSPO standards.

The economic benefits that development of oil palm brings to region needs to be accounted for when creating these thresholds. These benefits include an expanded corporate tax base at the national level. In addition, due to the manual labor associated with oil palm plantations, the United Nations Environment Program (UNEP) estimated one job created for every 2.3 ha of oil palm cultivation (UNEP 2011). The oil palm sector in Indonesia is estimated to provide full time employment for 3.8 million people (World Bank 2010). By 2012, Olam Gabon says that is has employed over 850 people in the region around the 51,000 ha Kango concession granted in 2010. However, there is some disagreement as to the economic benefits that oil palm development brings to local people (Obidzinski et al. 2012), although there is some evidence that much of the conflict over oil palm in local communities stems from a lack of transparency and consultation (Rist et al. 2010). Many of the negative economic impacts are based on the lost access and degradation of traditional land that provided benefits of forest resource extraction, hunting, water quality, etc. These issues are specifically addressed by RPSO standards (Rist et al. 2010). It should be noted that if much of Gabon is excluded from RSPO due

to carbon emissions from land-use change, the economic incentives for sustainable palm oil would be also be removed reducing incentives to meet these other socioeconomic standards for responsible development.

Deriving country- or region-specific guidelines and criteria are an important method forward to balance a nation's right to develop and expand their economies while maintaining standing forest cover. It is also possible to build flexibility into the standards as opposed to setting a strict threshold for carbon emissions. Many oil palm concessions, such as ML2 have large areas that are not suitable for oil palm development due to physical characteristics (e.g., slope, etc.) or environmental impacts in plantations interested in RPSO certification (e.g., great ape presence) and as a result are not developed. The carbon sequestion in these areas can be substantial. The AGB in logged Central African forests increases at a rate of $4.82 \pm 1.22$ Mg $ha^{-1}$ $yr^{-1}$ (Gourlet-Fleury et al. 2013). The carbon accounting time frame for standards to include maximum AGB of one oil palm stand rotation (approximately 20 yrs) would allow for the plateau forests of ML2 to increase by 1.4 Tg AGB or 0.7 Tg C. Thus credit for forest conservation could account for over 41% of the emissions from ML2. This figure could be improved even further through mitigation efforts of identifying hotspots of high carbon density in the heterogamous landscape to add to the conservation land. Maintaining standing plains forest above the $60^{th}$ percentile of carbon density would approximate no net emissions when accounting for projected AGB accumulation in ML2 standing forest over 20 years. It would require that an additional 3800 ha, or 21% of the plains, be conserved (Figure 18). There are dual benefits of conserving plains forests as it prevents immediate carbon emissions and increases the forested area sequestering carbon.

Understanding the spatial patterns and forest types in Gabon is important to prioritization and planning to mitigate emissions from development going forward. The future analysis of the national carbon assessment by land-use and type in Gabon will enable a comparison of this study in order to evaluate whether ML2 contains unusually high carbon stocks for degraded forests. This national assessment will play a key role going forward in terms of conservation planning and prioritization within Gabon. The field data from the assessment, augmented with LiDAR and land-use maps, will enable comprehensive planning in order to mitigate environmental impacts, including carbon emissions. A spatial and temporal understanding of the patterns in carbon density across the country would be beneficial in creating a long-term development plan for oil palm (and other agricultural sectors). Oil palm development is a vital part of Gabon's economic development plan and these results highlight the importance of identifying and prioritizing conservation areas with high carbon stocks while encouraging development in areas that are identified as degraded.

## 6. Acknowledgements

Olam Gabon funded the carbon assessment of Mouila Lot 2 through a grant to the Agence Nationale des Parcs Nationaux (ANPN). ANPN provided administrative and logistical support, as well as infrastructure, vehicles and equipment. The Nicholas School of the Environment Environmental Internship Fund (EIF) provided additional funding. Special thanks to Dr. Jennifer Swenson, Dr. Vincent Medjibe, Dr. Connie Clark, and Dr. Lee White for their insights and support for this project. In addition, thanks to the following ANPN staff who contributed to project implementation: J.-G. Diof, A. Maroga, C. Mbina, P. Nguema, A. Nkoghe Nze, M. Nziengui, C. Tayo, C. Tchambela, and A. Yebe. Thanks to the ANPN field technicians who collected the data in the field. Most importantly, thanks to Dr. John Poulsen for his support and invaluable insights.

# 7. Literature Cited


Agence Nationale des Parcs Nationaux. 2013. Gabon Forest Carbon Assessment: 1st Technical Report. 25 pgs.

Amigun, B, JK Musango, W Stafford. 2011. Biofuels and sustainability in Africa. *Renewable and Sustainable Energy Review*. 15: 1360-1372.

Aratrakorn, Sirirak, Somying Thunhikorn, and Paul F. Donaold. 2006. Changes in bird communities following conversion of lowland forest to oil palm and rubber plantation in southern Thailand. *Bird Conservation International*. 16: 71-82.

Asner, Gregory P., R. Flint Hughes, Peter M. Vitousek, David E. Knapp, Ty Kennedy-Bowdoin, Joseph Boardman, Roberta E. Martin, Michael Eastwood, and Robert O. Green. 2008. Invasive plants transform the three-dimensional structure of rain forests. *Proc. Natl. Acad. Sci. USA*. 105(11): 4519-4523.

Asner, Gregory P., George V.N. Powell, Joseph Mascaro, David E. Knapp, John K. Clark, et al. 2010. High-resolution forest carbon stocks and emissions in the Amazon. *Proc. Natl. Acad. Sci. USA*. 107(38). 16738-16742.

Baccini, A., Laporte, N., Goetz, S.J., Sun, M., and Dong, H. 2008. A first map of tropical Africa's above-ground biomass derived from satellite imagery. Environmental Research Letters 3. stacks.iop.org/ERL/3/045011

Berry, Nicholas J., Oliver L. Phillips, Simon L. Lewis, Jane K. Hill, David P. Edwards, et al. 2010. The high value of logged tropical forests: lessons from northern Borneo. *Biodiversity and Conservation*. 19: 985-997.

Carey, Andrew B., Mary Mae Hardt, Scott P. Horton, and Brian L. Biswell. 1991. Spring Bird Communities in the Oregon Coast Range. Pages 123-142. In Wildlife and Vegetation of Unmanaged Douglas-Fir Forests. Portland, OR: USDA Forest Service, Pacific Northwest Research Station. General Technical Report PNW-GTR 285.

Carlson, Kimberly M., Lisa M. Curran, Gregory P. Asner, Alice McDonald Pittman, Simon N. Trigg, and J. Marion Adeney. 2013. Carbon emissions from forest conversion by Kalimantan oil palm plantations. *Nature Climate Change*. 3: 283-287.

Chave, J., C. Andalo, S. Brown, M. A. Cairns, J. Q. Chambers, D. Eamus, H. Fölster, F. Fromard, N. Higuchi, T. Kira, J.-P. Lescure, B. W. Nelson, H. Ogawa, H. Puig, B. Riéra, and T. Yamakura. 2005. Tree Allometry and Improved Estimation of Carbon Stocks and Balance in Tropical Forests. *Oecologia*. 145: 87-99.

Clark, David B., Jane M. Read, Matthew L. Clark, Ana Murillo Cruz, Marianela Fallas Dotti, and Deborah A. Clark. 2004. Application of 1-m and 4-m resolution satellite data to ecological studies of tropical rain forests. *Ecological Applications.* 14(1): 61-74.

Clawges, Rick, Kerri Vierling, Lee Vierling, and Eric Rowell. 2008. The use of airborne lidar to assess avian species diversity, density, and occurance in a pine/aspen forest. *Remote Sensing of the Environment*. 112: 2064-2073.

Coops, Nicholas C., Thomas Hilker, Michael A. Wulder, Benoit St. Onge, Glenn Newnham, Anders Siggins, J.A. (Tony) Trofymow. 2007. Estimating canopy structure of Douglas-fir forest stands from discrete-return LiDAR. *Trees*. 21:295-310.

Daily, GC. 1995. Restoring value to the world's degraded lands. *Science*. 269: 350-354.

Danielsen F, Beukema H, Burgess ND et al. (2009) Biofuel plantations on forested lands: double jeopardy for biodiversity and climate. *Conservation Biology*. 23: 348-358.

Dixon RK, Brown S, Houghton RA, Solomon AM, Trexler MC, Wisniewski J. 1994. Carbon pools and flux of global forest ecosystems. *Science*. 263: 185-190.

Drake, Jason B., Ralph O. Dubayah, David B. Clark, Robert G. Knox, J. Bryan Blair, et al. 2002. Estimation of tropical forest structural characteristics using large-footprint lidar. *Remote Sensing of Environment*. 79: 305-319.

Ecosphere. 2013. Rapport préliminaire: Inventaire de flore pour la Concession du Lot 2 de Olam Gabon au Nord de Mouila.

Edwards, David P., Jenny Hodgson, Keith C. Hamer, Simon L. Mitchell, Abdul H. Ahmad, Stephen J. Cornell, and David S. Wilcove. 2010. Wildlife-friendly oil palm plantation fail to protect biodiversity effectively. *Conservation Letters*. 3(4): 236-242.

Environmental Systems Research Institute. 2013. ArcGIS Desktop: Release 10.2. Redlands, CA: Environmental Systems Research Institute.

Erdelen, Martin. 1984. Bird Communities and vegetation structure: I. Correlations and comparisons of simple and diversity indices. *Oecologia*. 61(2): 277-284.

FAO. 2010. FAOSTAT: Statistical Databases and Data-Sets. Food and Agriculture Organization of the UN. Rome, 12.

Fairhurst, T and D McLaughlin. 2009. Sustainable oil palm development on degraded land in Kalimantan. Washington, DC: World Wildlife Fund.

Fargione, J, J Hill, D Tilman, S Polasky, P Hawthorne. 2008. Land clearing and the biofuel carbon debt. *Science*. 319: 1235-1238.

Gautam, Sishir and Stephan A. Pietsch. 2012. Carbon Pools of an Intact Forest in Gabon. *African Journal of Ecology*. 50: 414-427.

Gibbs, H.K., A.S. Ruesch, F. Achard, M.K. Clayton, P. Holmgren, N. Ramankutty, and J.A. Foley. 2010. Tropical forests were the primary sources of new agricultural land in the 1980s and 1990s. *Proc. Natl. Acad. Sci. USA*. 107(38): 16732-16737.

Gonzalez, Patrick, Gregory P. Asner, John J. Battles, Michael A. Lefsky, Kristen M. Waring, and Michael Palace. 2010. Forest carbon densities and uncertainties from Lidar, QuickBird, and field measurements in California. *Remote Sensing of Environment*. 114(7): 1561-1575.

Gourlet-Fleury, Sylvie, Frédéric Mortier, Adeline Fayolle, Fidèle Baya, Dakis Ouédraogo, Fabrice Bénédet, and Nicolas Picard. 2013. Tropical forest recovery from logging: a 24 years silvicultural experiment from Central Africa. *Phil. Trans. R. Soc. B.* 368: 20120302.

Gullison, R.E., P.C. Frumhoff, J.G. Canadell, C.B. Field, D.C. Nepstad, K. Hayhoe, R. Avissar, L.M. Curran, P. Friedlingstein, C.D. Jones, and C. Nobre. 2007. Tropical forests and climate policy. *Science*. 316: 985-986.

Harris, Nancy L., Sandra Brown, Stephen C. Hagen, Sassan S. Saatchi, Silvia Petrova, William Salas, Matthew C. Hansen, Peter V. Potapov, and Alexander Lotsch. 2012. Baseline Map of Carbon Emissions from Deforestation in Tropical Regions. *Science*. 336: 1573-1576.

Hernandez-Aguilar, R. Adriana, Jim Moore, and Craig B. Stanford. 2013. Chimpanzee nesting patterns in savanna habitat: Envioronmental influences and preferences. *American Jounral of Primatology*. 75: 979-994.

Hijmans, R.J., S.E. Cameron, J.L. Parra, P.G. Jones and A. Jarvis. 2005. Very high resolution interpolated climate surfaces for global land areas. *International Journal of Climatology*. 25: 1965-1978.

Horne, Ross, and John Hickey. 1991. Ecological sensitivity of Australian rainforests to selective logging. *Australian Journal of Ecology*. 16: 119-129.

IUCN 2013. IUCN Red List of Threatened Species. Version 2013.2. <www.iucnredlist.org>.

IUCN SSC Primate Specialist Group. 2014. Industrial oil palm expansion in great ape habitat in Afria: A policy statement from the Section on Great Apes (SGA) of the IUCN SSC Primate Specialist Group. International Union for Conservation of Nature. http://www.primate-sg.org/storage/pdf/Statement_on_oil_palm_in_Africa.pdf

Jubanksi, J., U. Ballhorn, K. Kronseder, J. Franke, and F. Siegert. 2013. Detection of large above-ground biomass variability in lowland forest ecosystems by airborne LiDAR. *Biogeosciences*. 10: 3917-3930.

Kariuki, Maina, Robert M. Kooyman, R.G.B Smith, Grant Wardell-Johnson, and Jerome K. Vanclay. 2006. Regeneration changes in tree abundance , diversity and structure in logged and unlogged subtropical rainforest over a 36-year history. *Forest Ecology and Management*. 236: 162-176.

Koh, Lian Pin and David S. Wilcove. 2007. Cashing palm oil for conservation. *Nature*. 448: 993-994.

Koh, Lian Pin and David S. Wilcove. 2008. Is oil palm agriculture really destroying tropical biodiversity? *Conservation Letters*. 1: 60-64.

Koh, LP, J Miettinen, SC Liew, and J Ghazou. 2011. Reply to Paoli et al.: explicit consideration of model uncertainties. *Proceedings of the National Academy of Sciences of the United States of America.* 108: E219.

Koh, LP, P Levang, J Ghazoul. 2009. Designer landscapes for sustainable biofuels. *Trends in Ecology and Evolution* 24: 431-438.

Laporte, Nadine T., Jared A. Stabach, Robert Grosch, Tiffany S. Lin, and Scott J. Goetz. 2007. Expansion of industrial logging in Central Africa. *Science*. 316: 1451.

Laurance, William F., Thomas E. Lovejoy, Heraldo L. Vasconcelos, Emilio M. Bruna, Rapheal K. Didham, Philip C. Stouffer, Claude Gascon, Richard O. Bierregaard, Susan G. Laurance, and Erika Sampaio. 2002. Ecosystem Decay of Amazonian Forest Fragements: a 22-Year Investigation. *Conservation Biology*. 16(3): 605-618.

Lefsky, Michael A., Warren B. Cohen, Geoffrey G. Parker, and David J. Harding. 2002. Lidar remote sensing for ecosystem studies. *BioScience*. 52(1): 19-30.

Lefsky, Michael A., Andrew T. Hudak, Warren B. Cohen, and S.A. Acker. 2005. Geographic variability in lidar predications of forest stand structure in the Pacific Northwest. *Remote Sensing of Environment*. 95: 532-548.

Le Quéré, Corinne, Michael R. Raupach, Josep G. Canadell, Gregg Marland, Laurent Bopp, et al. 2009. Trends in the sources and sinks of carbon dioxide. *Nature Geoscience*. 2: 831-836.

Lesak, Adrian A. Volker C. Radeloff, Todd J. Hawbaker, Anna M. Pidgeon, Terje Gobakken, and Kirk Contrucci. 2011. Modeling forest songbird species richness using LiDAR-derived measures of forest structure. *Remote Sensing of the Environment*. 115: 2823-2835.

Lewis, Simon L., Gabriela Lopez-Gonzalez, Bonaventure Sonké, Kofi Affum-Baffoe, Timothy R. Baker, et al. 2009. Increasing carbon storage in intact African tropical forests. *Nature.* 457: 1003-1007.

Lewis, Simon L., Bonaventure Sonké, Terry Sunderland, Serge K. Begne, Gabriela Lopez-Gonzalez, et al. 2013. Above-ground biomass and structure of 260 African tropical forests. *Phil. Trans. R. Soc. B.* 368: 20120295.

Lim, Kevin, Paul Treitz, Michael Wulder, Benoît St-Onge, and Martin Flood. 2003. LiDAR remote sensing of forest structure. *Progress in Physical Geography*. 27(1): 88-106.

MacArthur, R.H., and J.W. MacArthur. 1961. On bird species diversity. *Ecology*. 42: 594-598

Malaysia Oil Palm Board. 2011. Available at <http://econ.mpob.gov.my/economy/annual/stat2011/EID_statistics2011.htm>

Medjibe, V. P., Francis E. Putz, and Claudia Romero. 2013. Certified and uncertified Logging Concessions Compared in Gabon: Changes in Stand Structure, Tree Species, and Biomass. *Environmental Management*. 51: 524-540.

Medjibe, Vincent P., Francis E. Putz, Malcolm P. Starkey, Auguste A. Ndouna, and Hervé R. Memiaghe. 2011. Impacts of selective logging on aboveground forest biomass in Monts de Cristal in Gabon. *Forest Ecology and Management.* 262: 1799-1806.

Meijaard, Erik, Damayanti Buchori, Yokyok Hadiprakarsa, Sri Suci Utami-Atmoko, Anton Nurcahyo, et al. 2011. Quantifying killing of orangutans and human-orangutan conflict in Kalimantan, Indonesia. *Plos One*. 6(11): e27491.

Meyer, V., S.S. Saatchi, J. Chave, J. Dalling, S. Bohlman, et al. 2013. Detecting tropical forest biomass dynamics from repeated airborne Lidar measurements. *Biogeosciences Discussions*. 10(2): 1957-1992.

Morel, Alexandra C., Sassan S. Saatchi, Yadvinder Malhi, Nicholas J. Berry, Lindsay Banin, et al. 2011. Estimating aboveground biomass in forest and oil palm plantation in Sabah, Malaysian Borneo using ALOS PALSAR data. *Forest Ecology and Management*. 262: 1786-1798.

Murcia, Carolina. 1995. Edge Effects in fragmented forests. *Trends in Ecology and Evolution*. 10(2): 58-62.

Nellemann, Christian, Lera Miles, Bjørn P. Kaltenborn, Melanie Virtue, and Hugo Ahlenius. (Eds.) 2007. The last stand of the orangutan – State of emergency: Illegal logging, fire, and palm oil in Indonesia's national parks. United Nations Enviornment Programme, GRID-Arendal, Norway.

Neves, F.S., K.S. Queiroz-Dantas, W.D. da Rocha, and J.H.C. Delabie. 2013. Ants of three adjacent habitats of a transition region between the Carrado and Caatinga biomes: The effects of heterogeneity and variation in canopy cover. *Neotropical Entomology*. 42(3):258-268.

Newell, Joshua P. and Robert O. Vos. 2012. Accounting for Forest Carbon Pool Dynamics in Product Carbon Footprints: Challenges and Opportunities. *Environmental Impact Assessment Review*.

Ngomanda, Alfred, Nestor Laurier Engone Obiang, Judicaël Lebamba, Quentin Moundounga Mavouroulou, Hugues Gomat, et al. 2014. Site-specific versus pantropical allometric equations: Which option to estimate the biomass of a moist central African forest? *Forest Ecology and Management.* 312: 1-9.

Obidzinski, K., R. Andriani, H. Komarudin, and A. Andrianto. 2012. Environmental and social impacts of oil palm plantations and their implications for biofuel production in Indonesia. *Ecology and Society* **17**(1): 25.

Olam. 2014. In a nutshell. Olamonline.com/about-us/in-a-nutshell/

Paoli, GD, KM Carlson, A Hooijer, et al. 2011. Policy perils of ignoring uncertainty in oil palm research. *Proceeding of the National Academy of Sciences of the United States of America*. 108.

Phillips, Oliver, Tim Baker, Ted Feldpausch, and Roel Brienen. 2009. RAINFOR Field Manual for Plot Establishment and Remeasurement.

Poulsen, John R., C.J. Clark, and B.M. Bolker. 2011. Decoupling the effects of logging and hunting on an Afrotropical animal community. *Ecological Applications*. 21(5): 1819-1836.

Poulsen, John R., Connie J. Clark, and Todd M. Palmer. 2013. Ecological erosion of an Afrotropical forest and potential consequences for tree recruitment and forest biomass. *Biological Conservation*. 163: 122-130.

Ramankutty, Navin, Holly K. Gibbs, Frédéric Achard, Ruth DeFries, Jonathan A. Foley, R.A. Houghton. 2007. Challenges to Estimating Carbon Emissions from Tropical Deforestation. *Global Change Biology*. 13: 51-66.

R Core Team (2013). R: A language and environment for statistical computing. R Foundation for Statistical Computing, Vienna, Austria. ISBN 3-900051-07-0, URL http://www.R-project.org/.

Rist, Lucy, Laurène Fientrenie, and Patrice Levang. 2012. The livelihood impacts of oil palm: smallholders in Indonesia. *Biodiveristy*. 19: 1009-9815.

Robertson, J.M. Yarrow and Carel P. van Schaik. 2001. Causal factors underlying the dramatic decline of the Sumatran orang-utan. *Oryx*. 35(1): 26-38.

RSPO. 2011. RSPO Greenhouse Gas Working Group 2: Outputs and Recommendations.

RSPO. 2013. Principles and Criteria for the production of Sustainable Palm Oil. Available at: <http://www.rspo.org/file/PnC_RSPO_Rev1.pdf>

Saatchi, S. S., N. L. Harris, S. Brown, M. Lefsky, E. T. a Mitchard, W. Salas, B. R. Zutta, W. Buermann, S. L. Lewis, S. Hagen, S. Petrova, L. White, M. Silman, and A. Morel. 2011. Benchmark map of forest carbon stocks in tropical regions across three continents. Proceedings of the National Academy of Sciences of the United States of America 108:9899–904.

Samson, D.R.,and KD Hunt. 2014. Chimpanzees Preferentially Select Sleeping Platform Construction Tree Species with Biomechanical Properties that Yield Stable, Firm, but Compliant Nests. PLoS ONE 9(4): e95361.

Saunders, Denis A., Richard J. Hobbs, and Chris R. Margules. 1991. Biological Consequences of Ecosystem Fragmentation: A Review. *Conservation Biology*. 5(1): 18-32.

van Schaik, Carel P., Kathryn A. Monk, and J.M. Yarrow Roberston. 2001. Dramatic decline in orang-utan numbers in the Leuser Ecosystem, Northern Sumatra. *Oryx*. 35(1): 14-25.

Senior, Michael J. M., Keith C. Hamer, Simon Bottrell, David P. Edwards, Tom M. Fayle, et al. Trait-dependent declines of species following conversion of rain forest to oil palm plantations. *Biodiversity Conservation*. 22: 253-268.

Sheil, DC, E Meijaard, M van Noordwijk, J Gaskell, J Sunderland-Groves, et al. 2009. The Impacts and opportunities of oil palm in Southeast Asia. Forestry CfI. Bogor, editor. CIFOR.

Souza, Alexandre F., Liseane Santos Rocha Cortez, and Solon Jonas Longhi. 2012. Native forest management in subtropical South America: long-term effects of logging and multiple-use on forest structure and diversity. *Biodiversity Conservation*. 21: 1953-1969.

Summary report of planning and management for Olam Palm Gabon, Mouila Lot 2: RSPO New Planting Procedures. 2013. Available at: <http://www.rspo.org/file/RSPO%20NPP%20SUMMARY%20OF%20PLANNING%20AND%20MANAGEMENT_OLAM%20PALM%20GABON_MOUILA%20LOT%202%282%29.pdf>

The Forests of the Congo Basin - State of the Forest 2010., Eds: C. de Wasseige, P. de Marcken, N. Bayol,F. Hiol Hio,Ph. Mayaux,B. Desclée,R. Nasi,A. Billand, P. Defourny, and R. Eba'a Atyi. 2012. Publications Office of the European Union. Luxembourg. 276 p. ISBN: 978-92-79-22716-5 , doi: 10.2788/47210

UNEP. 2011. Oil palm plantations: threats and opportunities for tropical ecosystems. Available at < http://www.unep.org/pdf/Dec_11_Palm_Plantations.pdf>

Venter, Oscar and Lian Pin Koh. 2012. Reducing emissions from deforestation and forest degradation (REDD+): Game changer or just another quick fix? *Annals of the New York Academy of Sciences*. 1249: 137-150.

Versi, Anver. 2012. Olam – The rewards of cleaner, greener investment. *African Business*. *Academic OneFile*.

Walsh, Peter D., Kate A. Abernethy, Magdalena Bermejo, Rene Beyers, Pauwei De Wachter, et al. 2003. Catastrophic ape decline in western equatorial Africa. *Nature*. 422: 611-614.

Wich, Serge A., David Gaveau, Nicola Abram, Marc Ancrenaz, Alessandro Baccini, et al. 2012. Understanding the Impacts of Land-Use Policies on a Threatened Species: Is there a Future for the Bornean Orang-utan? *Plos One*. 7(11): e49142.

Wilcove, Dave S. and Lian Pin Koh. 2010. Addressing the threats to biodiversity from oil-palm agriculture. *Biodiversity and Conversation.* 19: 99-1007.

World Bank. 2010. Boom, bust and up again? Evolution, Drivers and impact of commodity prices: Implications for Indonesia. World Bank, Jakarta.

Zanne, A.E., G. Lopez-Gonzalez, D.A. Coomes, J. Ilic, S. Jansen, S.L. Lewis, R.B. Miller, N.G. Swenson, M.C. Wiemann, and J. Chave. 2009. Global Wood Density Database. Dryad. <http://hdl.handle.net/10255/dryad.235>.

2nd Palm Oil Africa. 2013. Gabon – The next palm oil investment hub? <http://www.cmtevents.com/aboutevent.aspx?ev=131042>

# 8. Tables and Figures

Table 1. Comparison of plains plots (n=20) and HCVF plateau plots (n=10). In this comparison, we exclude plots 1 and 2, in which more than one third of their areas lacked stems ≥ 10 cm DBH. Here we present results from allometric equations that incorporate tree diameter, wood density and tree height (CMFH, NMFH) or just tree diameter and wood density (CMF, NMF).

| | **Plains** | **HCVF Plateau** | **95% CI** | **Statistic** | **p-value** |
|---|---|---|---|---|---|
| Biomass (Mg $ha^{-1}$) | | | | | |
| CMF | 310 | 387 | [-155.3,0.7] | $t_{13} = 2.14$ | p = 0.052 |
| CMFH | 257 | 346 | [-174.8,-2.2] | $t_{13} = 2.21$ | p = 0.045 |
| NMF | 243 | 301 | [-117.7,1.5] | $t_{13} = 2.10$ | p = 0.055 |
| NMFH | 212 | 282 | [-137.8,-1.6] | $t_{13} = 2.20$ | p = 0.046 |
| Height (meters) | 18.3 | 19.5 | [-6.3,2.7] | W = 73 | p = 0.436 |
| Per tree Basal Area ($cm^2$) | 587.1 | 595.8 | [-113.2,95.9] | $t_{22} = 0.171$ | p = 0.866 |
| Stem Count (stems $ha^{-1}$) | 421.6 | 498.7 | [-135.9,-18.4] | $t_{19} = 2.74$ | p = 0.012 |
| Plot Basal Area ($m^2$ $ha^{-1}$) | 24.1 | 29.6 | [-10.1,-0.9] | $t_{13} = 2.57$ | p = 0.023 |
| Wood Density (g $cm^{-3}$) | 0.666 | 0.646 | [-0.004,0.04] | $t_{26} = 1.702$ | p = 0.100 |

Table 2. Comparison of ABG and carbon in plains and plateau forest generated using the four field-based calculations and the two spatial AGB models (CMF = -36.199 + 16.277($Ht_{LiDAR}$), $R^2 = 0.798$, $F_{1, 28} = 112.9$, $p < 0.001$; CMFH = -23.341 + 13.542($Ht_{LiDAR}$), $R^2 = 0.522$, $F_{1, 28} = 32.67$, $p < 0.001$).

| Type | Equation | Plains | | Plateau | | Estimated Emissions |
|---|---|---|---|---|---|---|
| | | Tg AGB | Tg C | Tg AGB | Tg C | Tg C |
| **Field** | **CMF** | 5.09 | 2.54 | 5.47 | 2.73 | 1.66 |
| **Model** | **CMF** | 4.86 | 2.43 | 5.26 | 2.63 | 1.54 |
| **Field** | **CMFH** | 4.22 | 2.11 | 4.88 | 2.44 | 1.22 |
| **Model** | **CMFH** | 4.15 | 2.08 | 4.48 | 2.24 | 1.19 |
| **Field** | **NFM** | 3.99 | 1.99 | 4.25 | 2.12 | 1.10 |
| **Field** | **NFMH** | 3.47 | 1.74 | 3.97 | 1.99 | 0.85 |

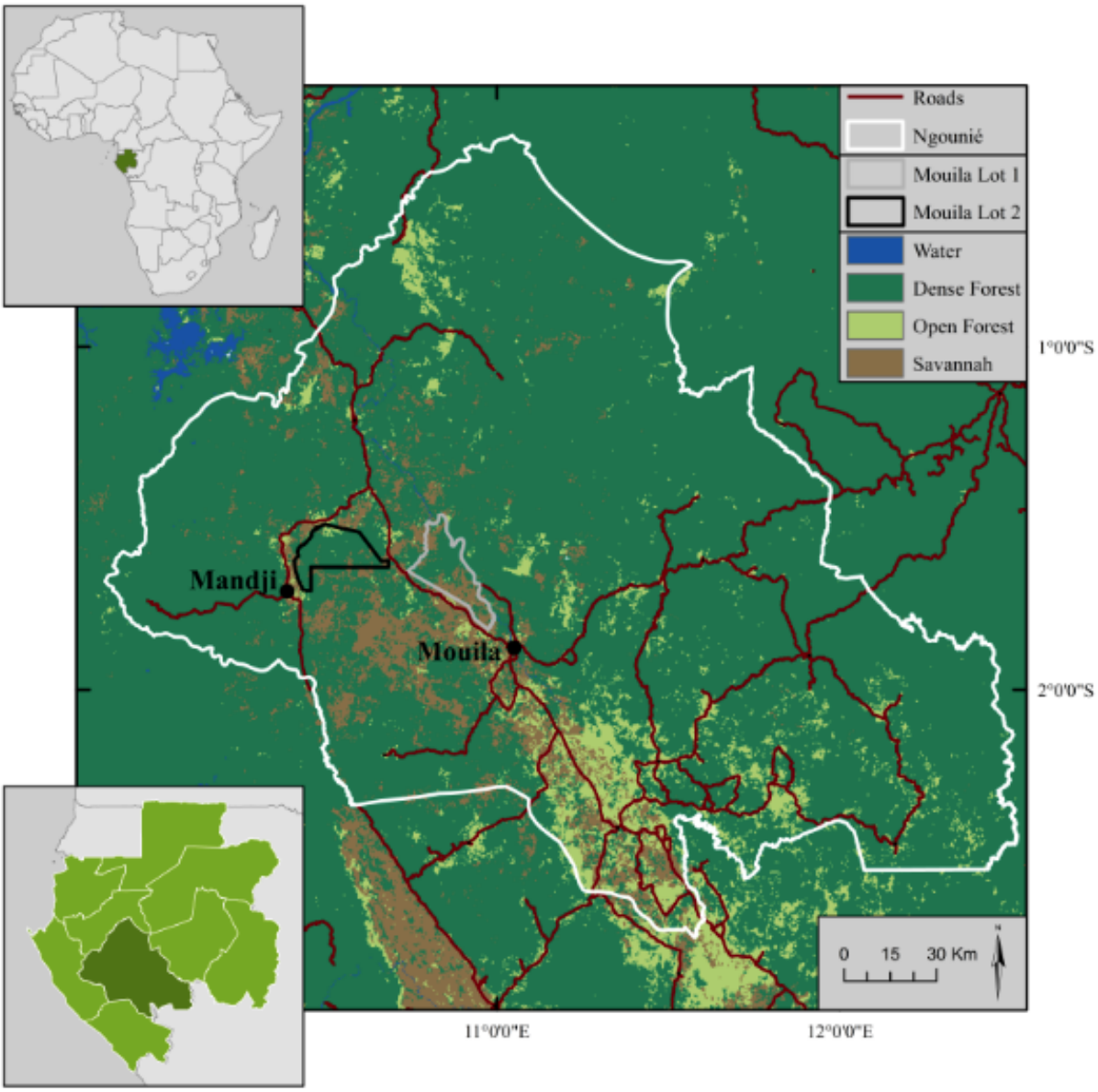


Figure 1. The Mouila Concession, Lot 1 and 2, in the Ngounié Province of Gabon, Africa. Upper left inset map depicts the location of Gabon within Africa. Lower left inset map shows the location of the Ngounié Province within Gabon.

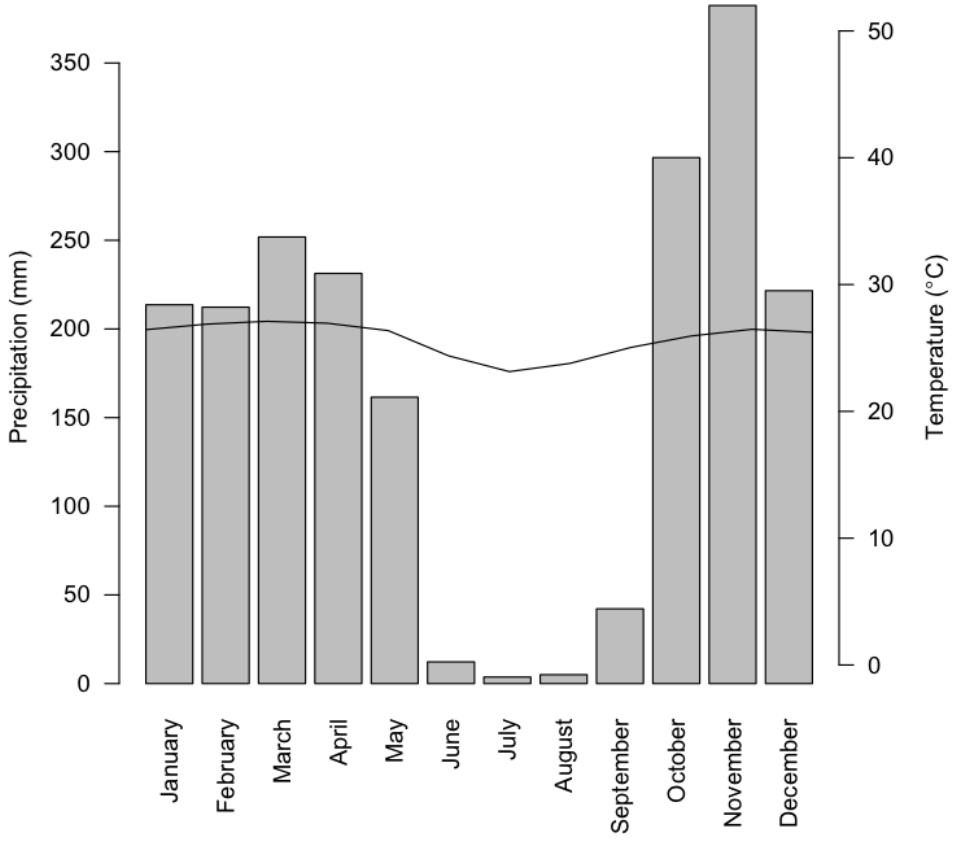


Figure 2. Monthly climate data for the ML2 concession in Gabon. Bars show monthly precipitation (mm) and line shows temperature (°C). Figure constructed using data interpolated from climate stations with data from 1950 – 2000 by WorldClim – Global Climate Data (Hijmans 2005).

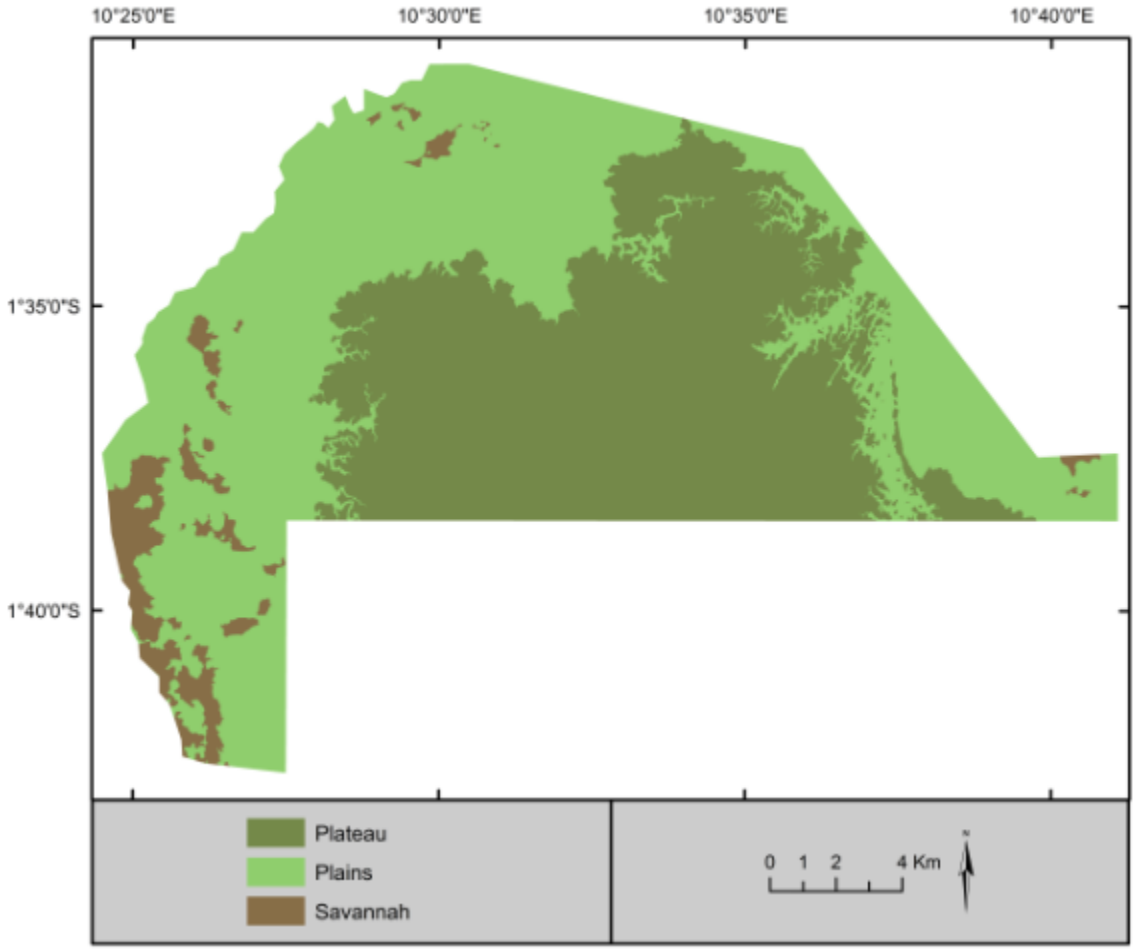


Figure 3. The principal habitat types within ML2, including plateau (High Value Conservation Forest set-asides), plains, and savannah. Oil palm development will occur in plains and savannah area.

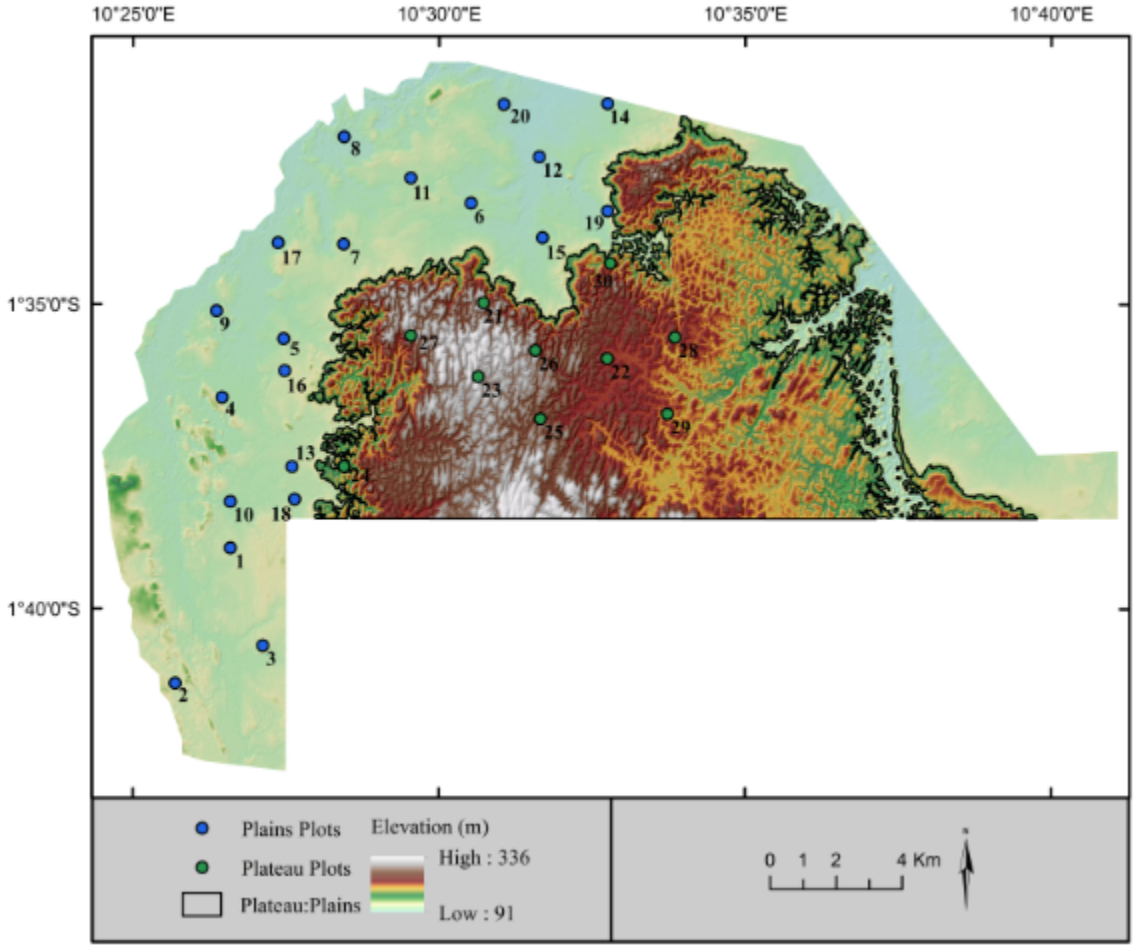


Figure 4. Spatial layout of 30 1-ha plots within the ML2 concession.

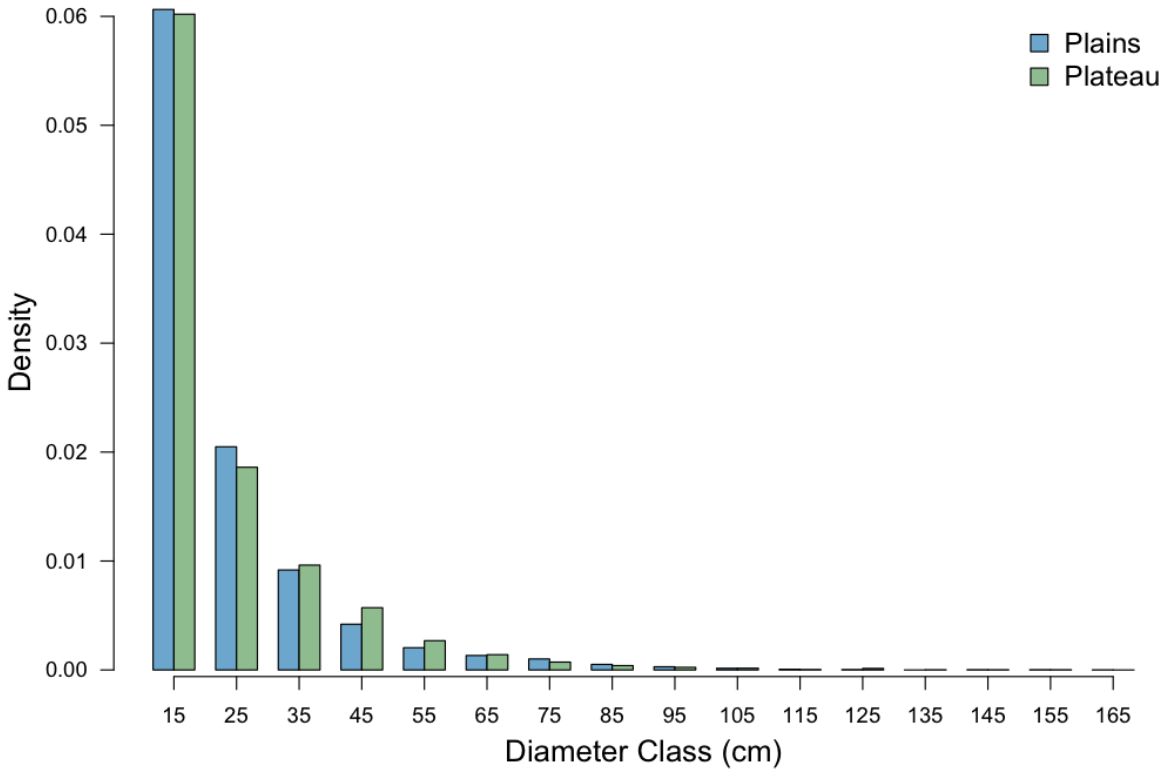


Figure 5. Stem diameters for individual trees on the plains and the plateau, respectively, were from different distributions ($D = 0.027$, $p = 0.026$). Labels are the center of each diameter class (e.g., 15 represents all stems with a diameter from 10-20 cm).

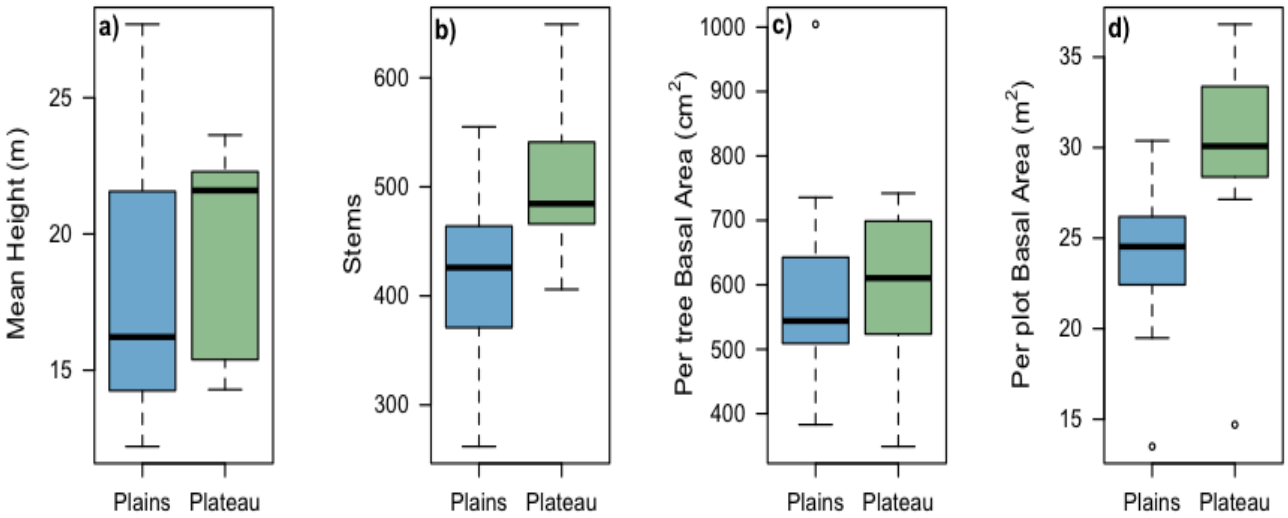


Figure 6. Comparison of a) mean tree height ($W$ =73, $p$ = 0.436), b) stem count ($t_{19}$ = 2.74, $p$ = 0.012), c) per tree basal area ($t_{22}$ = 0.171, $p$ = 0.866), and d) per plot basal area ($t_{13}$ = 2.57, $p$ = 0.023) for plots located in the plains and plateau forests. In this comparison, we exclude plots 1 and 2, in which more than one third of their areas lacked stems ≥ 10 cm DBH. Boxes indicate the interquartile range (IQR) with whiskers extended to the most extreme value within 1.5 times the IQR. Open circles represent data values outside this range.

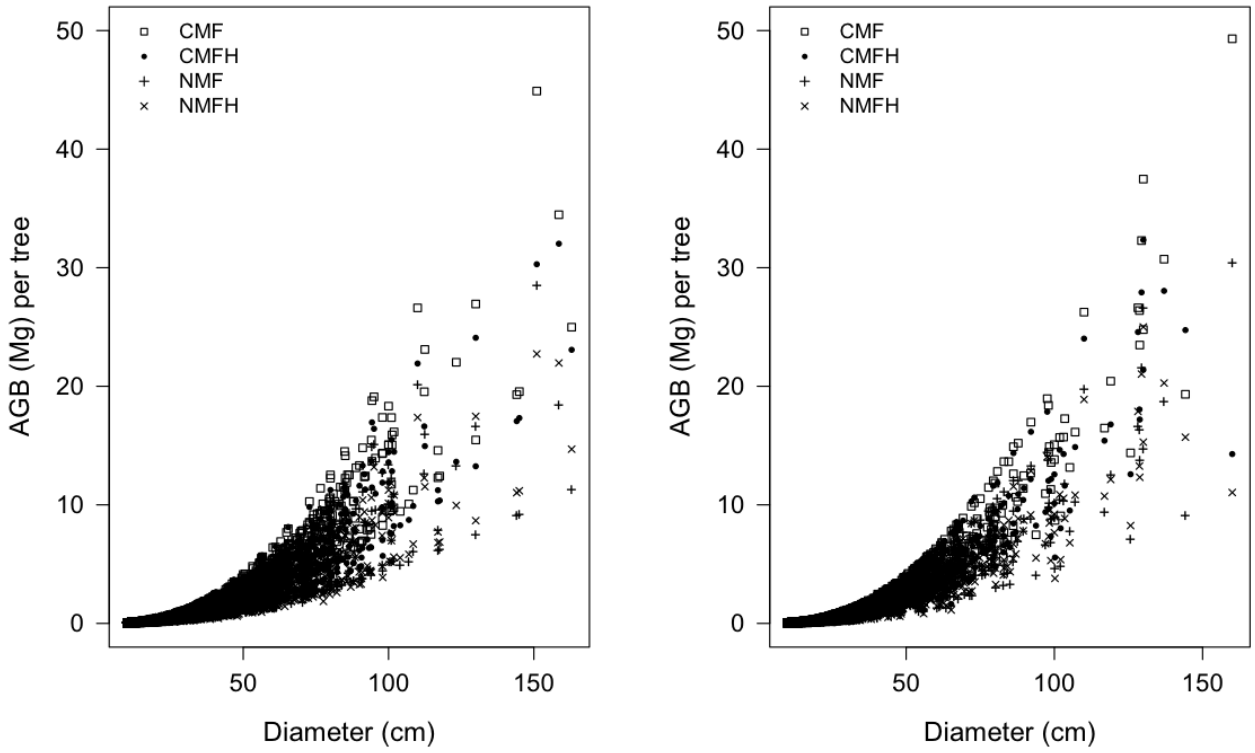


Figure 7. Comparison of AGB allometric equations. Chave Moist (CMF) and Ngomanda (NMF) allometric equations incorporating information on tree diameters and species-specific wood densities without and with a height variable (CMFH and NMFH, respectively) were used to evaluate the per tree AGB across the range of diameters for plains (left) and plateau forests (right).

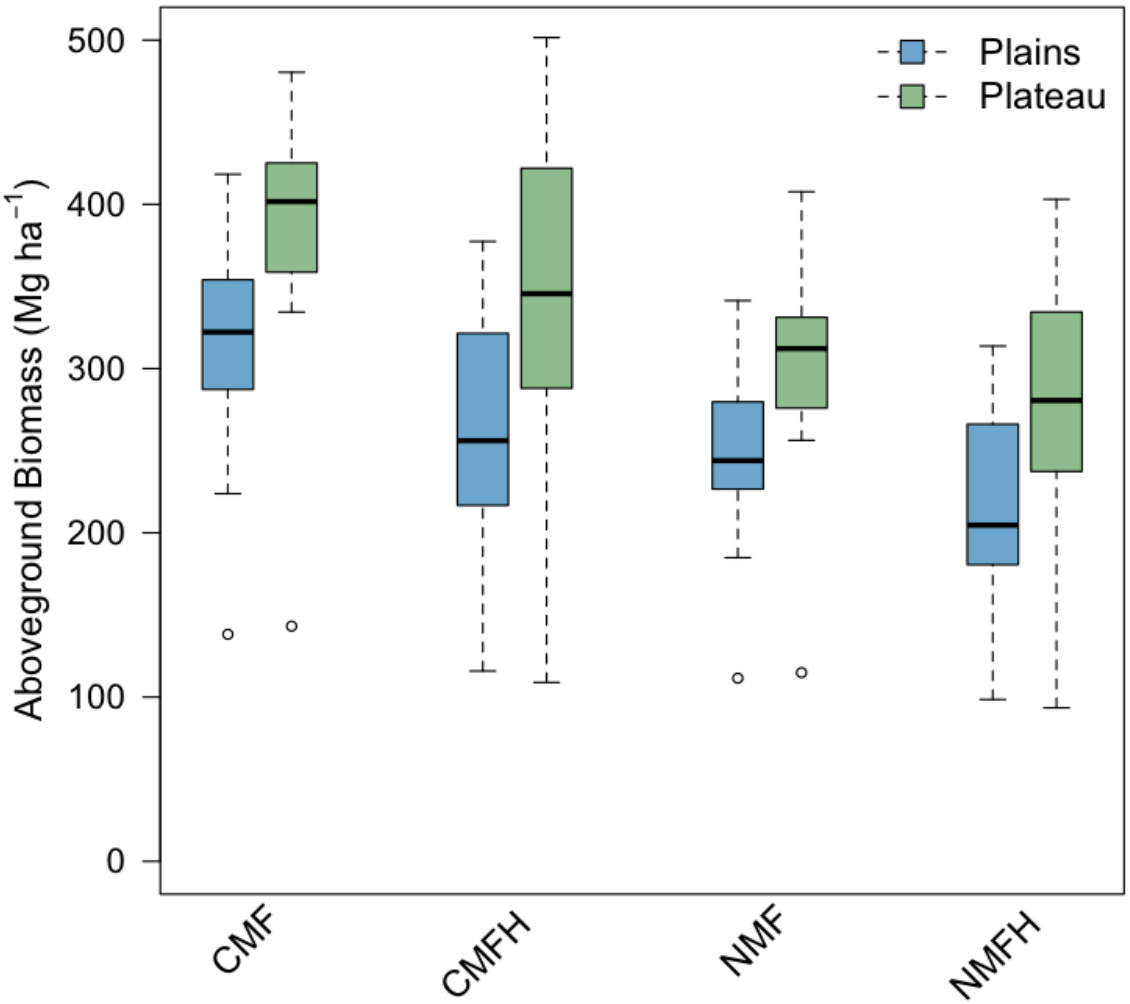


Figure 8. Biomass (Mg ha$^{-1}$) comparisons between plains and plateau plots using the Chave Moist (CMF) and Ngomanda (NMF) allometric equations incorporating diameter and species-specific wood density without and with a height variable (CMFH and NMFH, respectively). In this comparison, we exclude plots 1 and 2, in which more than one third of their areas lacked stems ≥ 10 cm DBH. There was no significant difference between plains and plateau forest plots using CMF ($t_{13} = 2.14$, $p = 0.052$) and NMF ($t_{13} = 2.10$, $p = 0.055$) without height. However, the plateau forests did have significantly higher biomass values than plains forest plots for both CMFH ($t_{13} = 2.21$, $p = 0.045$) and NMFH ($t_{13} = 2.20$, $p = 0.046$) when a height variable was included. Boxes indicate the interquartile range (IQR) with whiskers extended to the most extreme value within 1.5 times the IQR. Open circles represent data values outside this range.

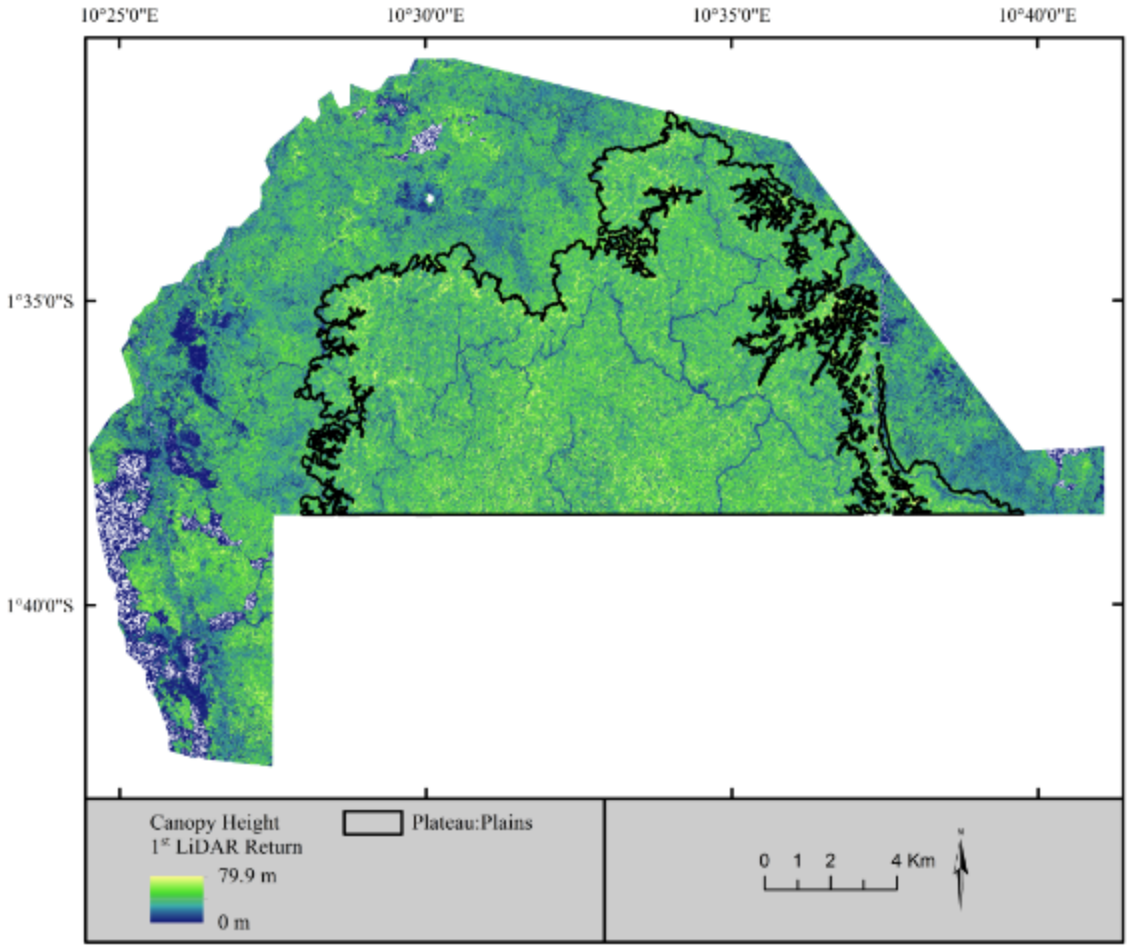


Figure 9. The canopy height model for ML2 derived from the LiDAR 1st return dataset.

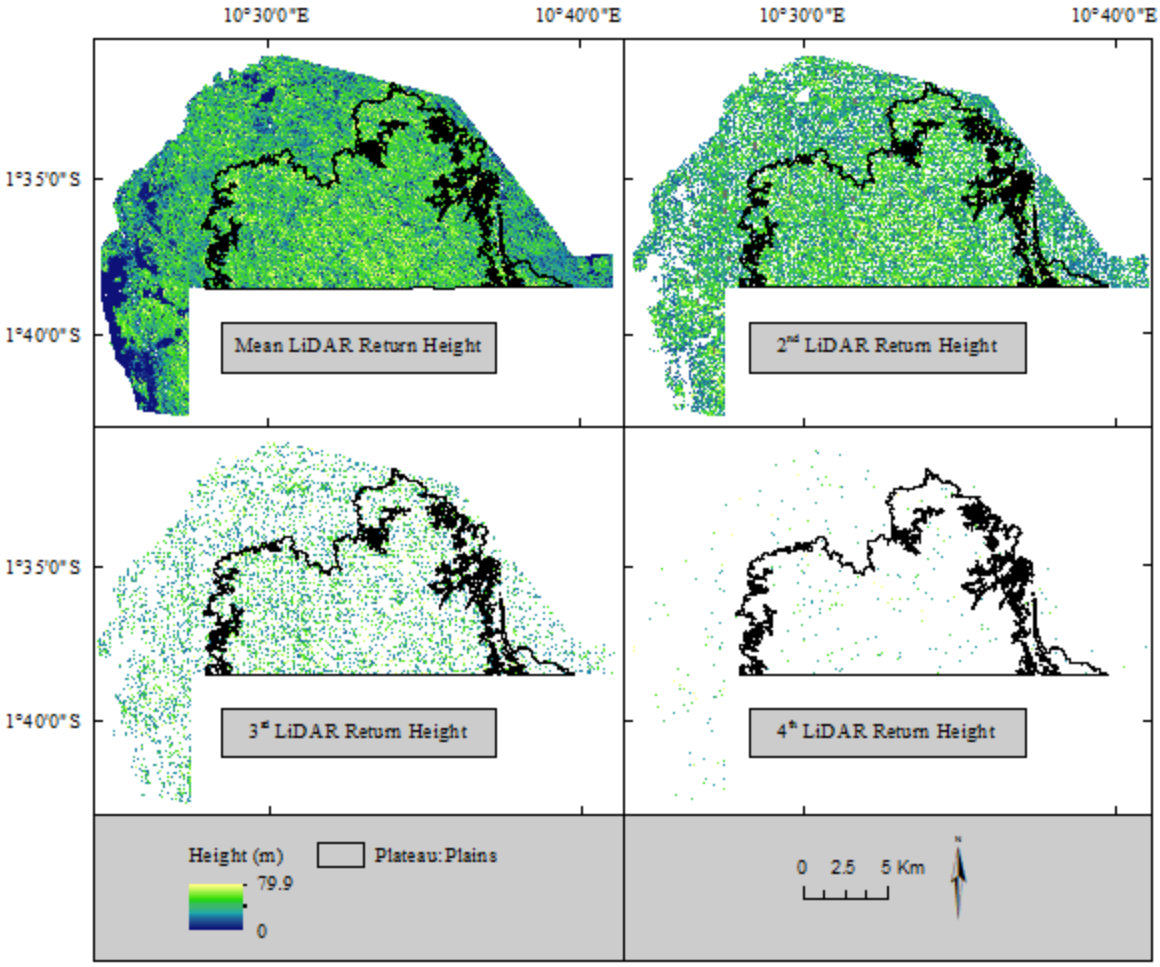


Figure 10. Spatial model of the LiDAR heights from all, second, third and fourth returns. These inputs, combined with the first returns,were used to derive the plot-based LiDAR metrics to predict spatially explicit carbon densities across ML2.

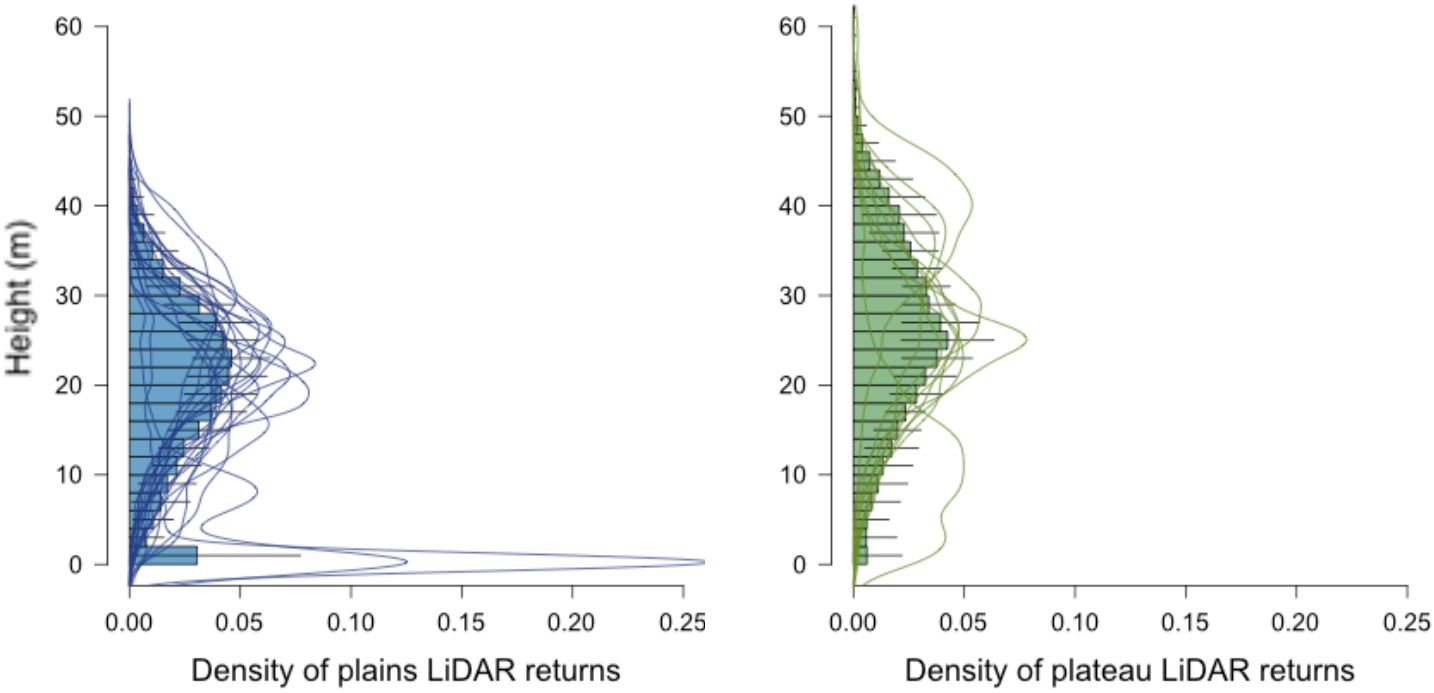


Figure 11. The vertical canopy height profiles from LiDAR in the ML2 plots. Bars represent the cumulative LiDAR heights for the plateau and plains plots, respectively. The density distribution curves show individual plot returns.

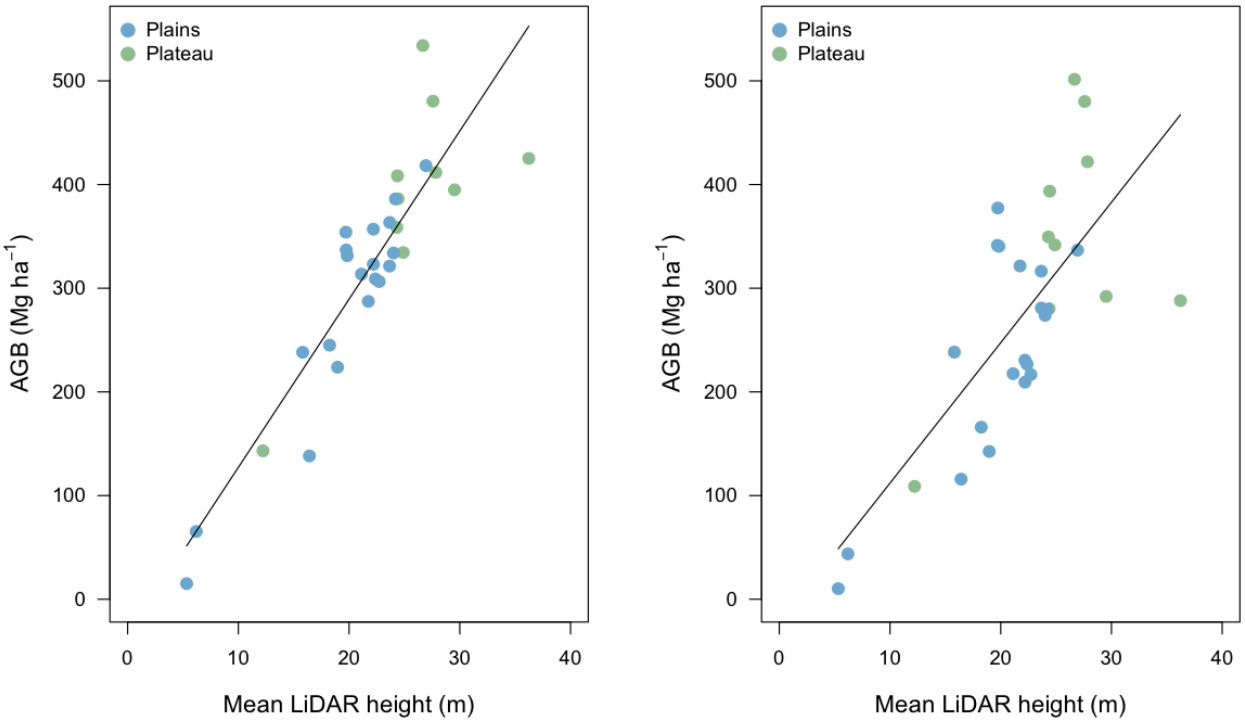


Figure 12. Regression models of mean biomass from field measurements and mean LiDAR canopy return height. LiDAR height explained a significant amount of the variability in AGB calculated from both the CMF (left) and CMFH (right) allometric equations (CMF = -36.199 + 16.277($Ht_{LiDAR}$), $R^2 = 0.798$, $F_{1, 28} = 112.9$, $p < 0.001$; CMFH = -23.341 + 13.542($Ht_{LiDAR}$), $R^2 = 0.522$, $F_{1, 28} = 32.67$, $p < 0.001$).

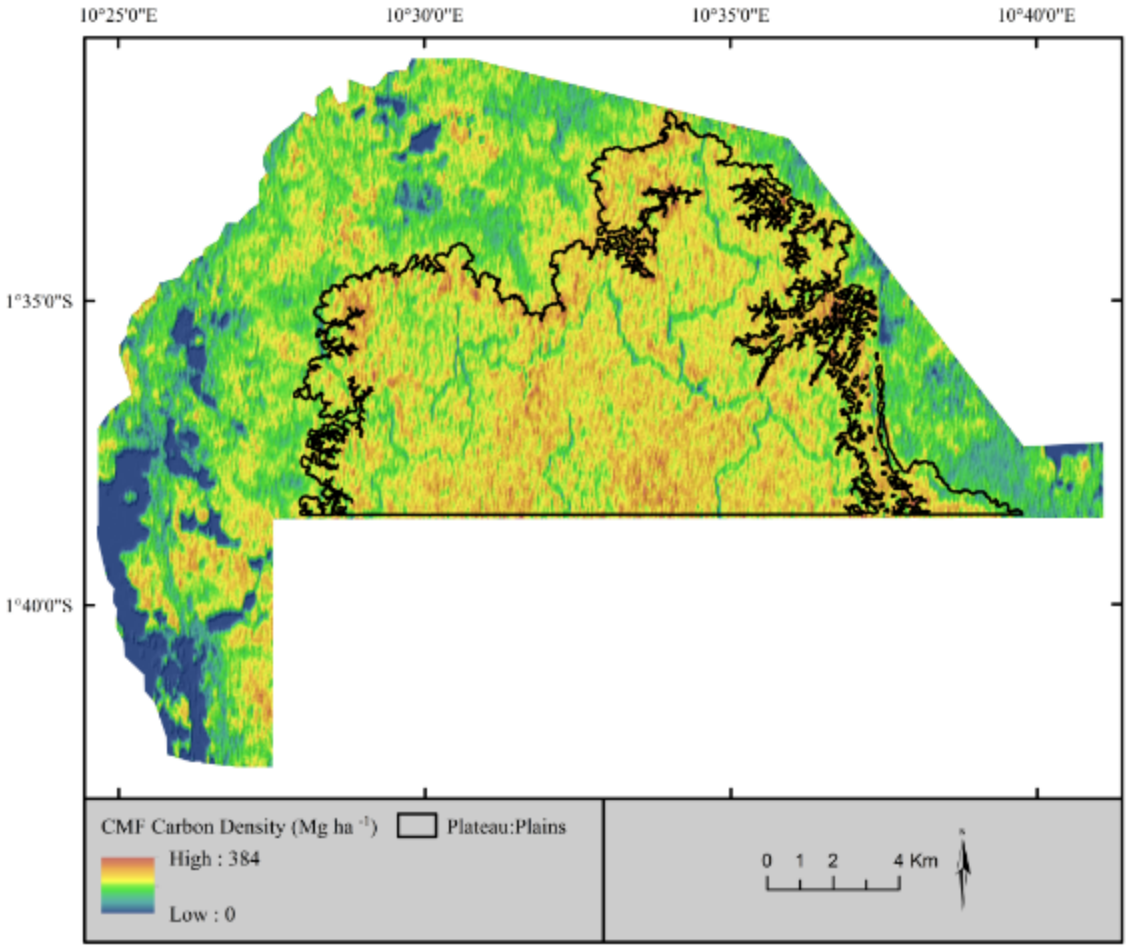


Figure 13. Spatial model of carbon density across ML2 using the CMF allometric equation.

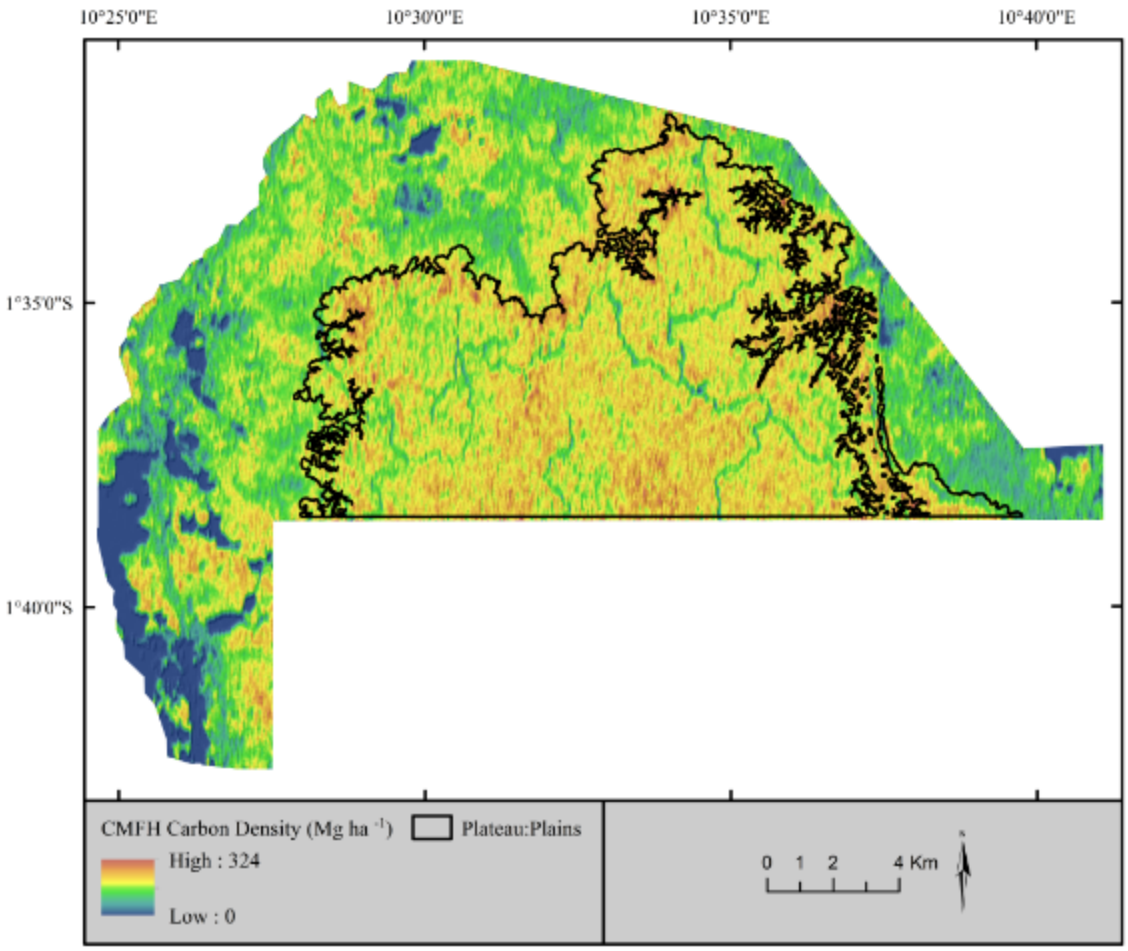


Figure 14. Spatial model of carbon density across the ML2 using the CMFH (incorporating tree heights) allometric equation.

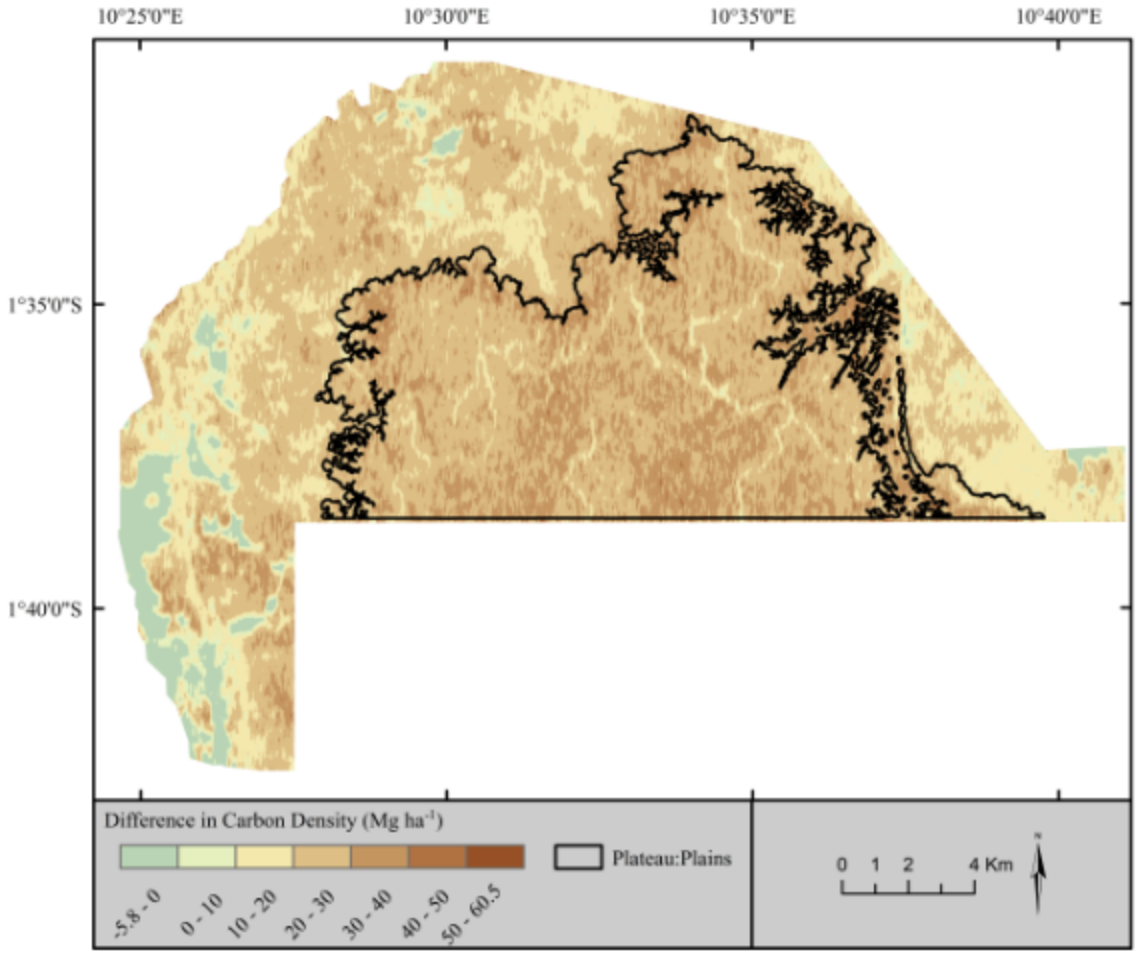


Figure 15. Spatially explicit distribution of the difference in carbon density between the CMF and CMFH (incorporating tree heights) models.

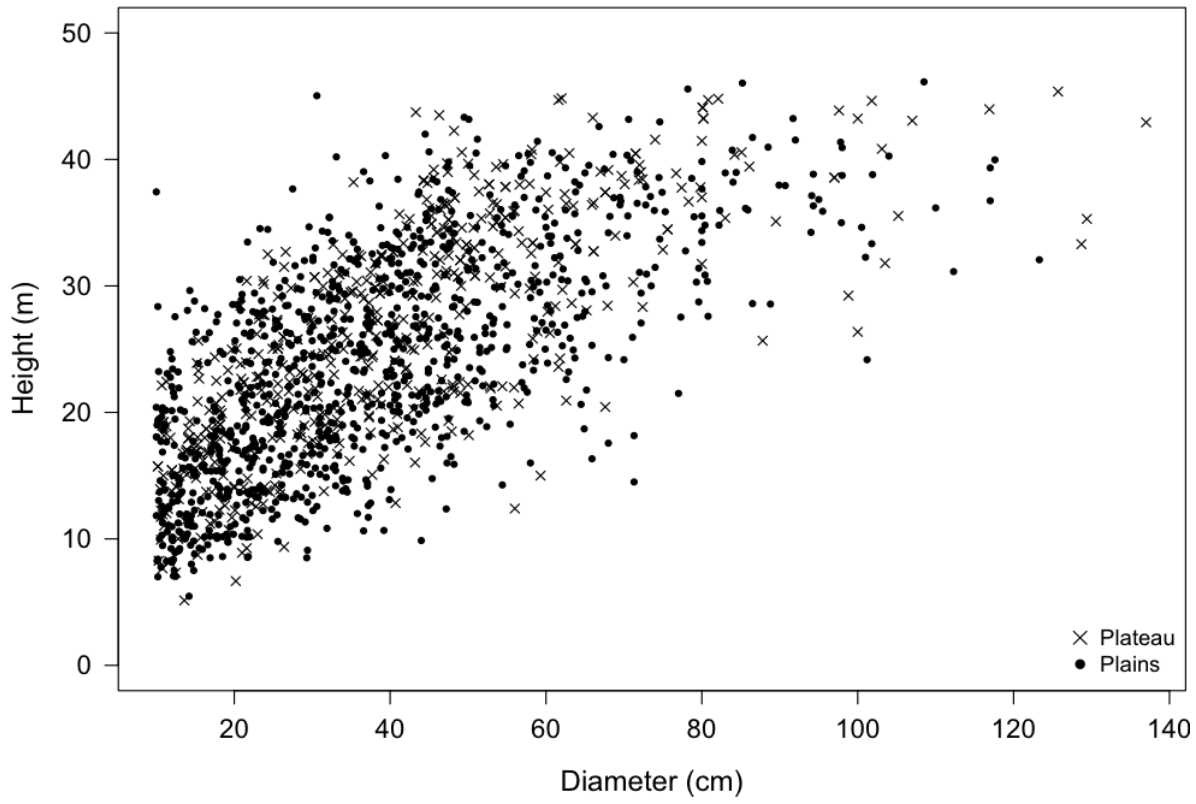


Figure 16. The relationship between height and diameter of tree stems measured in the field.

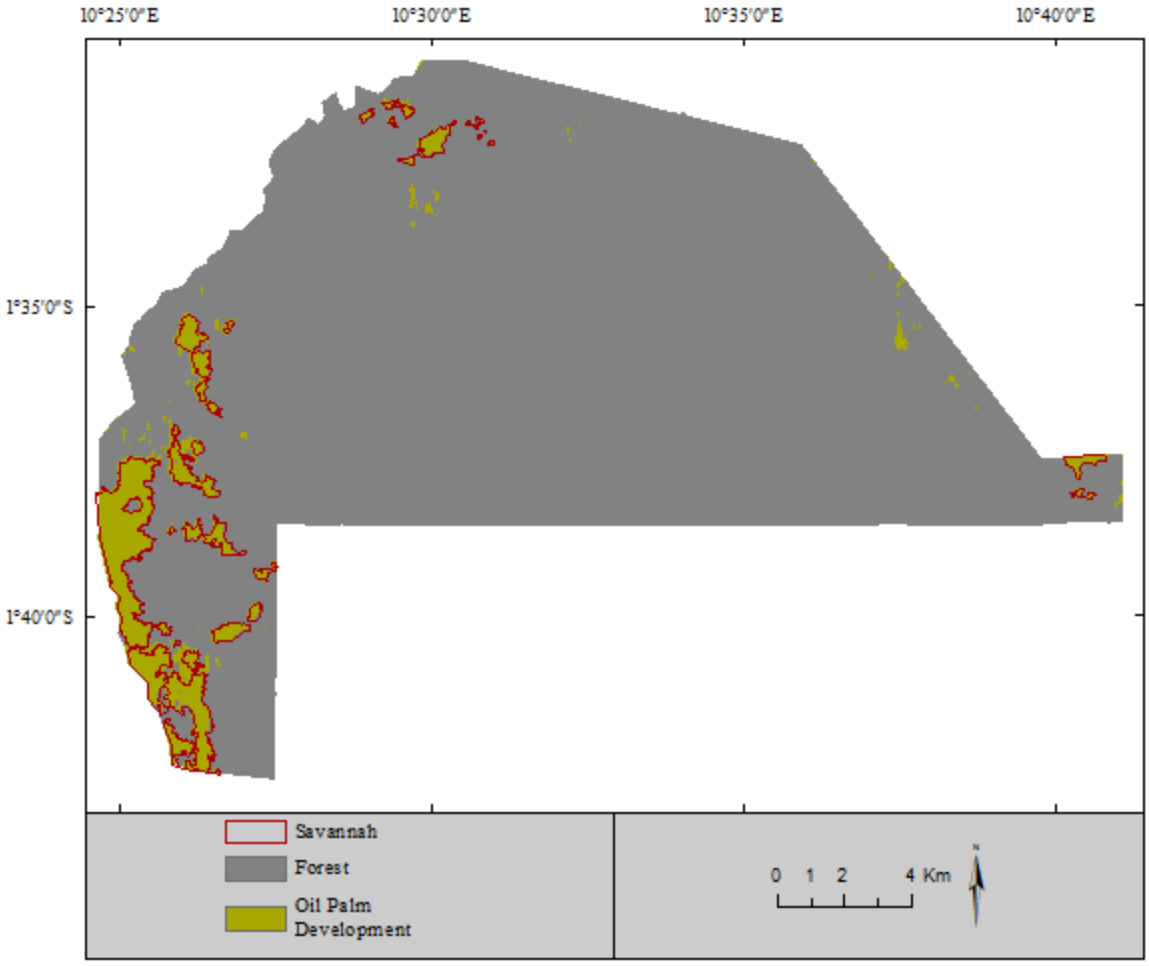


Figure 17. Spatially explicit distribution of the area in ML2 plains that could be converted to oil palm with no net carbon emissions using the CMFH spatial model.

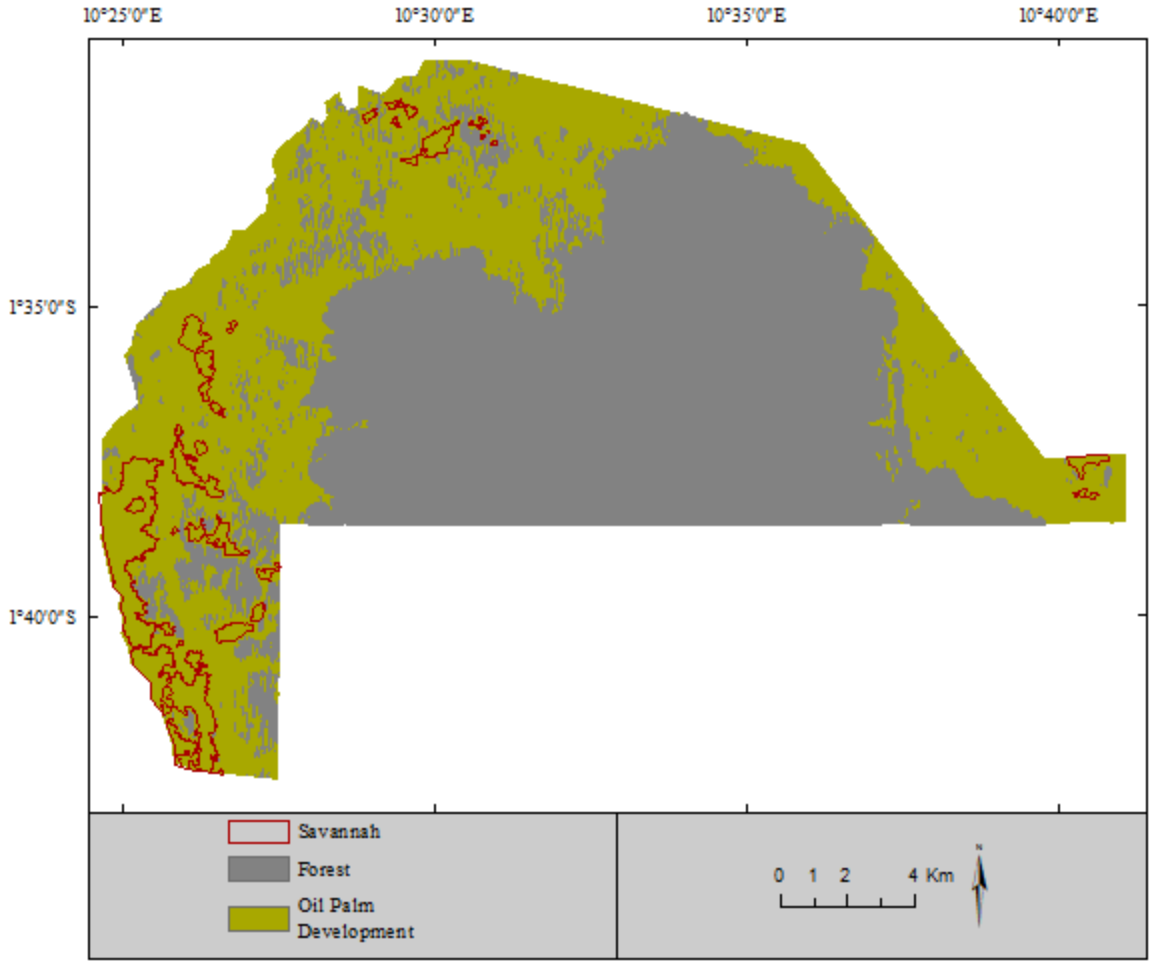


Figure 18. Spatially explicit distribution of the area in ML2 plains that could be converted to oil palm with no net carbon emissions using the CMFH spatial model when accounting for 20 years of AGB accumulation in ML2's standing forests.

# 9. Appendix

Appendix A. Forest characteristics for each of the 30 plots in the Mouila Lot 2 Concession.

| Plot | Type | Stem Count | Mean Height (m) | Median Height (m) | SD Height (m) | Mean Diameter (cm) | Median Diameter (cm) | SD Diameter (cm) | Mean Basal Area ($cm^2$) | Median BA ($cm^2$) | SD BA ($cm^2$) | Plot Basal Area ($m^2$) | **Aboveground Biomass (Mg $ha^{-1}$)** | | | |
|---|---|---|---|---|---|---|---|---|---|---|---|---|---|---|---|---|
| | | | | | | | | | | | | | Chave Moist | Chave Moist Height | Ngomanda | Ngomanda Height |
| 1 | Plains | 52 | 12.04 | 10.61 | 4.56 | 18.41 | 14.70 | 11.02 | 359.67 | 169.75 | 520.35 | 1.87 | 15.03 | 10.20 | 10.86 | 8.32 |
| 2 | Plains | 194 | 14.69 | 13.70 | 2.77 | 18.35 | 14.25 | 12.21 | 380.81 | 159.49 | 720.47 | 7.39 | 65.37 | 43.75 | 45.56 | 35.19 |
| 3 | Plains | 262 | 18.76 | 17.10 | 6.06 | 26.72 | 19.00 | 23.82 | 1004.41 | 283.53 | 2459.65 | 26.32 | 333.96 | 273.82 | 226.64 | 208.27 |
| 4 | Plains | 333 | 17.91 | 16.93 | 3.78 | 20.16 | 16.60 | 10.47 | 405.21 | 216.42 | 458.83 | 13.49 | 138.23 | 115.86 | 111.49 | 98.51 |
| 5 | Plains | 342 | 14.78 | 14.40 | 4.91 | 25.05 | 18.60 | 16.14 | 696.82 | 271.72 | 913.48 | 23.83 | 356.92 | 230.61 | 301.71 | 197.23 |
| 6 | Plains | 359 | 24.26 | 21.90 | 5.38 | 24.27 | 18.00 | 17.99 | 716.05 | 254.47 | 1361.72 | 25.71 | 321.32 | 316.46 | 238.54 | 252.16 |
| 7 | Plains | 371 | 15.38 | 13.99 | 4.47 | 23.79 | 19.00 | 15.26 | 626.88 | 283.53 | 1046.87 | 23.26 | 306.43 | 216.72 | 245.36 | 180.58 |
| 8 | Plains | 388 | 13.75 | 12.05 | 4.54 | 23.72 | 18.45 | 16.02 | 642.76 | 267.35 | 1241.46 | 24.94 | 323.13 | 209.39 | 245.57 | 171.15 |
| 9 | Plains | 399 | 14.24 | 12.84 | 4.07 | 22.30 | 17.90 | 13.36 | 530.39 | 251.65 | 792.60 | 21.16 | 245.06 | 165.98 | 193.61 | 138.60 |
| 10 | Plains | 407 | 16.35 | 13.92 | 5.46 | 24.32 | 16.80 | 18.61 | 735.64 | 221.67 | 1392.36 | 29.94 | 386.09 | 279.36 | 279.71 | 222.29 |
| 11 | Plains | 424 | 14.25 | 13.87 | 2.69 | 21.61 | 19.00 | 10.89 | 459.51 | 283.53 | 554.50 | 19.48 | 223.83 | 142.57 | 184.85 | 123.88 |
| 12 | Plains | 428 | 16.09 | 14.48 | 5.16 | 22.91 | 17.40 | 15.96 | 611.79 | 237.79 | 1191.96 | 26.18 | 363.45 | 280.90 | 285.20 | 231.09 |
| 13 | Plains | 442 | 26.34 | 25.55 | 4.68 | 22.26 | 18.80 | 12.48 | 511.31 | 277.59 | 692.05 | 22.60 | 287.31 | 321.44 | 239.06 | 270.82 |
| 14 | Plains | 444 | 12.20 | 10.23 | 5.62 | 21.07 | 15.90 | 14.13 | 505.05 | 198.56 | 919.69 | 22.42 | 313.60 | 217.58 | 255.22 | 182.81 |
| 15 | Plains | 461 | 20.44 | 18.71 | 7.16 | 22.41 | 17.50 | 13.99 | 547.78 | 240.53 | 916.85 | 25.25 | 354.04 | 341.37 | 292.16 | 286.55 |
| 16 | Plains | 464 | 27.70 | 26.84 | 4.86 | 21.66 | 16.60 | 14.79 | 539.99 | 216.42 | 967.31 | 25.06 | 336.94 | 377.38 | 270.48 | 313.72 |
| 17 | Plains | 474 | 13.70 | 12.11 | 5.51 | 21.12 | 16.45 | 14.23 | 509.07 | 212.53 | 955.91 | 24.13 | 309.04 | 226.68 | 242.62 | 187.60 |
| 18 | Plains | 504 | 26.60 | 25.41 | 3.95 | 22.48 | 16.45 | 16.21 | 602.76 | 212.53 | 1275.86 | 30.38 | 331.36 | 340.41 | 232.27 | 266.14 |
| 19 | Plains | 531 | 15.84 | 14.06 | 5.60 | 21.65 | 16.50 | 14.82 | 540.17 | 213.83 | 972.87 | 28.68 | 418.28 | 336.68 | 341.39 | 281.82 |
| 20 | Plains | 555 | 21.56 | 20.20 | 3.99 | 18.90 | 15.60 | 11.43 | 382.93 | 191.13 | 738.78 | 21.25 | 238.17 | 238.38 | 189.46 | 201.10 |
| 21 | Plateau | 473 | 22.29 | 19.56 | 7.69 | 24.83 | 18.10 | 16.81 | 705.69 | 257.30 | 1201.28 | 33.38 | 411.65 | 421.98 | 311.75 | 334.47 |
| 22 | Plateau | 406 | 15.39 | 12.30 | 5.86 | 24.23 | 18.45 | 17.42 | 699.03 | 267.35 | 1448.86 | 28.38 | 408.41 | 280.28 | 312.55 | 229.55 |
| 23 | Plateau | 421 | 15.75 | 15.33 | 3.37 | 18.72 | 15.90 | 9.70 | 349.10 | 198.56 | 445.04 | 14.70 | 143.16 | 108.89 | 114.87 | 93.46 |
| 24 | Plateau | 466 | 23.63 | 20.94 | 5.89 | 22.60 | 16.75 | 15.21 | 582.48 | 220.36 | 1017.90 | 27.14 | 334.42 | 341.75 | 256.31 | 276.06 |
| 25 | Plateau | 470 | 14.72 | 13.46 | 4.95 | 23.68 | 17.95 | 16.42 | 651.65 | 253.06 | 1163.03 | 30.63 | 425.17 | 288.01 | 331.23 | 237.35 |
| 26 | Plateau | 496 | 21.83 | 19.16 | 6.34 | 25.04 | 19.10 | 17.85 | 742.18 | 286.52 | 1509.27 | 36.81 | 534.10 | 501.54 | 407.67 | 403.04 |
| 27 | Plateau | 519 | 22.13 | 20.51 | 7.59 | 22.64 | 17.00 | 14.57 | 569.09 | 226.98 | 939.18 | 29.54 | 386.28 | 393.57 | 307.86 | 323.26 |
| 28 | Plateau | 541 | 23.55 | 21.33 | 5.60 | 23.25 | 17.40 | 16.53 | 638.58 | 237.79 | 1260.71 | 34.55 | 480.40 | 480.11 | 373.81 | 389.80 |
| 29 | Plateau | 546 | 14.29 | 11.72 | 5.25 | 21.31 | 15.35 | 14.59 | 523.55 | 185.06 | 911.34 | 28.59 | 394.91 | 292.06 | 319.96 | 243.91 |
| 30 | Plateau | 649 | 21.36 | 18.76 | 5.46 | 21.30 | 16.00 | 13.37 | 496.47 | 201.06 | 854.72 | 32.22 | 358.69 | 349.47 | 275.93 | 285.06 |

Appendix B. LiDAR height characteristics for canopy returns for each of the 30 plots in the Mouila Lot 2 Concession. All values in meters.

| | | Return 1 | | | | | Return 2 | | | | | Return 3 | | | | | Return 4 | | | | | Cumulative Returns | | | | |
|---|---|---|---|---|---|---|---|---|---|---|---|---|---|---|---|---|---|---|---|---|---|---|---|---|---|---|
| Plot | Type | Min. | Max. | Range | Mean | SD | Min. | Max. | Range | Mean | SD | Min. | Max. | Range | Mean | SD | Min. | Max. | Range | Mean | SD | Min. | Max. | Range | Mean | SD |
| 1 | Plains | 0.00 | 42.50 | 42.50 | 8.49 | 11.54 | 0.00 | 35.49 | 36.09 | 10.02 | 9.41 | 0.00 | 35.25 | 35.70 | 9.50 | 8.96 | 0.00 | 18.11 | 18.42 | 5.63 | 5.74 | 0.00 | 39.33 | 39.33 | 5.33 | 9.07 |
| 2 | Plains | 0.00 | 40.28 | 40.27 | 8.63 | 8.16 | 0.00 | 33.22 | 34.02 | 5.96 | 6.23 | 0.00 | 25.86 | 26.51 | 4.76 | 6.31 | 0.00 | 17.51 | 17.76 | 5.36 | 5.64 | 0.00 | 36.91 | 36.91 | 6.20 | 7.05 |
| 3 | Plains | 0.15 | 49.60 | 49.45 | 26.67 | 11.51 | 0.00 | 41.44 | 42.44 | 15.51 | 9.60 | 0.00 | 40.16 | 41.19 | 11.18 | 9.50 | 0.00 | 29.73 | 30.10 | 6.84 | 8.54 | 0.00 | 45.54 | 45.54 | 24.01 | 10.54 |
| 4 | Plains | 0.22 | 36.00 | 35.78 | 17.41 | 7.66 | 0.00 | 27.94 | 29.12 | 10.13 | 6.66 | 0.00 | 26.72 | 27.64 | 6.25 | 6.04 | 0.00 | 16.66 | 16.94 | 3.83 | 4.95 | 0.04 | 34.43 | 34.39 | 16.42 | 7.24 |
| 5 | Plains | 2.76 | 41.61 | 38.85 | 23.56 | 5.81 | 0.00 | 34.97 | 35.57 | 14.35 | 7.04 | 0.00 | 27.93 | 28.55 | 6.97 | 6.62 | 0.00 | 20.94 | 20.98 | 4.93 | 5.52 | 2.64 | 42.58 | 39.94 | 22.19 | 5.76 |
| 6 | Plains | 1.71 | 45.12 | 43.42 | 26.58 | 7.83 | 0.00 | 36.19 | 36.57 | 15.55 | 7.93 | 0.00 | 35.58 | 36.33 | 10.75 | 7.97 | 0.00 | 27.10 | 27.46 | 7.70 | 7.75 | 0.00 | 40.11 | 40.11 | 23.66 | 7.02 |
| 7 | Plains | 2.48 | 47.84 | 45.36 | 24.12 | 8.42 | 0.00 | 44.26 | 45.09 | 15.99 | 8.29 | 0.00 | 37.81 | 38.48 | 10.92 | 8.85 | 0.00 | 25.32 | 25.67 | 4.65 | 7.40 | 2.32 | 47.41 | 45.09 | 22.72 | 8.08 |
| 8 | Plains | 0.09 | 42.24 | 42.15 | 23.69 | 7.90 | 0.00 | 38.39 | 39.12 | 15.35 | 8.11 | 0.00 | 30.52 | 31.38 | 9.71 | 8.06 | 0.00 | 21.34 | 21.58 | 4.09 | 5.81 | 0.00 | 39.62 | 39.62 | 22.19 | 7.47 |
| 9 | Plains | 0.87 | 43.59 | 42.73 | 19.67 | 8.01 | 0.00 | 35.86 | 36.41 | 12.48 | 7.85 | 0.00 | 34.59 | 35.16 | 8.54 | 7.80 | 0.00 | 13.92 | 14.25 | 6.47 | 4.88 | 0.26 | 40.75 | 40.49 | 18.24 | 7.37 |
| 10 | Plains | 0.32 | 48.09 | 47.77 | 26.31 | 7.95 | 0.00 | 40.32 | 40.98 | 16.09 | 8.64 | 0.00 | 32.84 | 34.03 | 9.25 | 7.68 | 0.18 | 18.00 | 17.82 | 3.43 | 4.27 | 0.00 | 45.54 | 45.54 | 24.19 | 7.71 |
| 11 | Plains | 0.41 | 34.06 | 33.66 | 20.01 | 5.88 | 0.00 | 26.74 | 27.70 | 11.36 | 6.52 | 0.00 | 23.70 | 24.75 | 5.92 | 6.37 | 0.00 | 7.80 | 8.15 | 1.56 | 2.25 | 0.00 | 33.41 | 33.41 | 18.96 | 5.80 |
| 12 | Plains | 0.58 | 39.96 | 39.38 | 25.31 | 6.61 | 0.00 | 36.18 | 36.70 | 15.63 | 7.04 | 0.00 | 31.14 | 31.97 | 8.76 | 7.30 | 0.00 | 22.26 | 22.71 | 2.99 | 5.02 | 0.76 | 39.55 | 38.79 | 23.67 | 6.38 |
| 13 | Plains | 0.47 | 36.40 | 35.93 | 23.01 | 6.12 | 0.00 | 31.10 | 32.29 | 13.42 | 7.74 | 0.00 | 27.09 | 27.62 | 7.30 | 7.03 | 0.00 | 6.45 | 6.60 | 1.26 | 2.35 | 1.02 | 35.50 | 34.48 | 21.74 | 6.09 |
| 14 | Plains | 0.39 | 40.96 | 40.57 | 22.57 | 9.06 | 0.00 | 36.60 | 37.04 | 13.56 | 8.75 | 0.00 | 32.35 | 32.92 | 8.00 | 7.74 | 0.00 | 14.55 | 15.12 | 3.08 | 4.83 | 0.00 | 39.43 | 39.43 | 21.12 | 8.41 |
| 15 | Plains | 0.06 | 43.10 | 43.04 | 21.16 | 8.38 | 0.00 | 35.91 | 36.80 | 13.04 | 8.30 | 0.00 | 38.08 | 38.90 | 8.60 | 7.87 | 0.00 | 21.41 | 21.93 | 8.18 | 8.43 | 0.00 | 40.89 | 40.89 | 19.71 | 8.24 |
| 16 | Plains | 0.18 | 37.21 | 37.03 | 21.34 | 7.45 | 0.00 | 31.77 | 32.71 | 13.08 | 6.50 | 0.00 | 27.54 | 28.40 | 8.06 | 6.53 | 0.00 | 15.49 | 16.14 | 3.86 | 5.01 | 0.00 | 35.92 | 35.92 | 19.74 | 7.16 |
| 17 | Plains | 2.56 | 45.15 | 42.59 | 24.50 | 8.93 | 0.00 | 41.50 | 41.91 | 15.51 | 7.90 | 0.00 | 36.86 | 37.86 | 9.94 | 7.49 | 0.00 | 28.36 | 29.29 | 5.28 | 6.23 | 2.64 | 43.30 | 40.66 | 22.38 | 8.14 |
| 18 | Plains | 0.15 | 37.42 | 37.27 | 21.42 | 6.47 | 0.00 | 34.00 | 34.67 | 13.17 | 6.93 | 0.00 | 26.04 | 26.86 | 8.16 | 6.82 | 0.56 | 16.48 | 15.92 | 5.49 | 5.15 | 0.15 | 36.81 | 36.66 | 19.83 | 6.03 |
| 19 | Plains | 2.32 | 45.05 | 42.73 | 29.02 | 8.40 | 0.00 | 42.00 | 42.46 | 17.51 | 8.49 | 0.00 | 31.98 | 32.71 | 10.41 | 8.13 | 0.00 | 20.10 | 20.85 | 5.74 | 6.89 | 0.16 | 45.18 | 45.02 | 26.94 | 8.35 |
| 20 | Plains | 0.06 | 40.20 | 40.15 | 17.30 | 8.28 | 0.00 | 35.33 | 36.18 | 10.89 | 6.78 | 0.00 | 25.63 | 26.65 | 7.44 | 6.05 | 0.00 | 11.91 | 12.77 | 3.31 | 4.06 | 0.00 | 37.31 | 37.31 | 15.81 | 7.68 |
| 21 | Plateau | 6.45 | 50.28 | 43.83 | 30.98 | 7.69 | 0.00 | 40.62 | 41.01 | 21.11 | 7.78 | 0.00 | 44.10 | 45.23 | 15.90 | 9.09 | 0.00 | 32.78 | 34.33 | 11.18 | 9.19 | 4.16 | 44.14 | 39.98 | 27.83 | 7.08 |
| 22 | Plateau | 0.40 | 48.70 | 48.31 | 26.33 | 8.90 | 0.00 | 43.41 | 44.49 | 17.04 | 9.27 | 0.00 | 38.72 | 39.48 | 11.71 | 9.24 | 0.00 | 23.91 | 24.72 | 7.54 | 8.06 | 0.29 | 46.25 | 45.96 | 24.37 | 8.58 |
| 23 | Plateau | 0.00 | 48.25 | 48.25 | 13.73 | 9.57 | 0.00 | 41.58 | 42.64 | 7.72 | 7.14 | 0.00 | 38.86 | 39.79 | 4.83 | 5.77 | 0.00 | 21.41 | 21.75 | 3.15 | 5.15 | 0.00 | 45.11 | 45.11 | 12.22 | 8.96 |
| 24 | Plateau | 0.55 | 67.08 | 66.53 | 27.16 | 10.61 | 0.00 | 59.02 | 60.55 | 17.90 | 10.29 | 0.00 | 45.75 | 49.78 | 11.85 | 9.95 | 0.00 | 28.67 | 29.30 | 5.39 | 7.24 | 0.00 | 62.72 | 62.72 | 24.89 | 10.29 |
| 25 | Plateau | 0.34 | 58.74 | 58.40 | 39.89 | 8.83 | 0.00 | 48.31 | 49.58 | 25.24 | 10.26 | 0.00 | 46.27 | 48.68 | 16.81 | 11.07 | 0.00 | 32.38 | 32.61 | 9.85 | 10.20 | 0.00 | 56.97 | 56.97 | 36.23 | 8.49 |
| 26 | Plateau | 0.11 | 57.07 | 56.96 | 29.06 | 9.64 | 0.00 | 50.05 | 52.10 | 19.57 | 9.79 | 0.00 | 46.88 | 48.99 | 14.88 | 11.35 | 0.00 | 38.55 | 40.36 | 9.63 | 10.51 | 0.00 | 55.40 | 55.40 | 26.66 | 9.30 |
| 27 | Plateau | 2.16 | 44.32 | 42.16 | 25.59 | 6.53 | 0.00 | 38.17 | 39.33 | 17.53 | 8.01 | 0.00 | 35.37 | 36.46 | 9.39 | 8.52 | 0.15 | 13.03 | 12.88 | 2.69 | 3.73 | 2.80 | 42.24 | 39.44 | 24.42 | 6.18 |
| 28 | Plateau | 1.13 | 49.68 | 48.55 | 30.15 | 9.73 | 0.00 | 43.80 | 44.78 | 19.76 | 9.29 | 0.00 | 44.71 | 45.74 | 12.41 | 9.54 | 0.00 | 26.12 | 26.73 | 5.86 | 6.07 | 0.78 | 48.27 | 47.49 | 27.58 | 9.44 |
| 29 | Plateau | 2.21 | 49.30 | 47.09 | 31.97 | 9.83 | 0.00 | 44.38 | 45.25 | 20.32 | 10.75 | 0.00 | 40.80 | 42.09 | 11.65 | 9.80 | 0.00 | 23.01 | 23.26 | 8.22 | 8.42 | 1.60 | 48.40 | 46.80 | 29.52 | 9.74 |
| 30 | Plateau | 0.61 | 48.44 | 47.83 | 25.75 | 7.83 | 0.00 | 44.44 | 46.01 | 17.31 | 8.93 | 0.00 | 40.24 | 41.04 | 10.39 | 8.74 | 0.00 | 27.46 | 27.48 | 7.54 | 7.71 | 0.26 | 46.89 | 46.63 | 24.31 | 7.94 |

Appendix B cont. LiDAR height characteristics for canopy returns for each of the 30 plots in the Mouila Lot 2 Concession. All values in meters.

| | | Return 1 | | | | | Return 2 | | | | | Return 3 | | | | | Return 4 | | | | | Cumulative Returns | | | | |
|---|---|---|---|---|---|---|---|---|---|---|---|---|---|---|---|---|---|---|---|---|---|---|---|---|---|---|
| Plot | Type | Min. | Max. | Range | Mean | SD | Min. | Max. | Range | Mean | SD | Min. | Max. | Range | Mean | SD | Min. | Max. | Range | Mean | SD | Min. | Max. | Range | Mean | SD |
| 1 | Plains | 0.00 | 42.50 | 42.50 | 8.49 | 11.54 | 0.00 | 35.49 | 36.09 | 10.02 | 9.41 | 0.00 | 35.25 | 35.70 | 9.50 | 8.96 | 0.00 | 18.11 | 18.42 | 5.63 | 5.74 | 0.00 | 39.33 | 39.33 | 5.33 | 9.07 |
| 2 | Plains | 0.00 | 40.28 | 40.27 | 8.63 | 8.16 | 0.00 | 33.22 | 34.02 | 5.96 | 6.23 | 0.00 | 25.86 | 26.51 | 4.76 | 6.31 | 0.00 | 17.51 | 17.76 | 5.36 | 5.64 | 0.00 | 36.91 | 36.91 | 6.20 | 7.05 |
| 3 | Plains | 0.15 | 49.60 | 49.45 | 26.67 | 11.51 | 0.00 | 41.44 | 42.44 | 15.51 | 9.60 | 0.00 | 40.16 | 41.19 | 11.18 | 9.50 | 0.00 | 29.73 | 30.10 | 6.84 | 8.54 | 0.00 | 45.54 | 45.54 | 24.01 | 10.54 |
| 4 | Plains | 0.22 | 36.00 | 35.78 | 17.41 | 7.66 | 0.00 | 27.94 | 29.12 | 10.13 | 6.66 | 0.00 | 26.72 | 27.64 | 6.25 | 6.04 | 0.00 | 16.66 | 16.94 | 3.83 | 4.95 | 0.04 | 34.43 | 34.39 | 16.42 | 7.24 |
| 5 | Plains | 2.76 | 41.61 | 38.85 | 23.56 | 5.81 | 0.00 | 34.97 | 35.57 | 14.35 | 7.04 | 0.00 | 27.93 | 28.55 | 6.97 | 6.62 | 0.00 | 20.94 | 20.98 | 4.93 | 5.52 | 2.64 | 42.58 | 39.94 | 22.19 | 5.76 |
| 6 | Plains | 1.71 | 45.12 | 43.42 | 26.58 | 7.83 | 0.00 | 36.19 | 36.57 | 15.55 | 7.93 | 0.00 | 35.58 | 36.33 | 10.75 | 7.97 | 0.00 | 27.10 | 27.46 | 7.70 | 7.75 | 0.00 | 40.11 | 40.11 | 23.66 | 7.02 |
| 7 | Plains | 2.48 | 47.84 | 45.36 | 24.12 | 8.42 | 0.00 | 44.26 | 45.09 | 15.99 | 8.29 | 0.00 | 37.81 | 38.48 | 10.92 | 8.85 | 0.00 | 25.32 | 25.67 | 4.65 | 7.40 | 2.32 | 47.41 | 45.09 | 22.72 | 8.08 |
| 8 | Plains | 0.09 | 42.24 | 42.15 | 23.69 | 7.90 | 0.00 | 38.39 | 39.12 | 15.35 | 8.11 | 0.00 | 30.52 | 31.38 | 9.71 | 8.06 | 0.00 | 21.34 | 21.58 | 4.09 | 5.81 | 0.00 | 39.62 | 39.62 | 22.19 | 7.47 |
| 9 | Plains | 0.87 | 43.59 | 42.73 | 19.67 | 8.01 | 0.00 | 35.86 | 36.41 | 12.48 | 7.85 | 0.00 | 34.59 | 35.16 | 8.54 | 7.80 | 0.00 | 13.92 | 14.25 | 6.47 | 4.88 | 0.26 | 40.75 | 40.49 | 18.24 | 7.37 |
| 10 | Plains | 0.32 | 48.09 | 47.77 | 26.31 | 7.95 | 0.00 | 40.32 | 40.98 | 16.09 | 8.64 | 0.00 | 32.84 | 34.03 | 9.25 | 7.68 | 0.18 | 18.00 | 17.82 | 3.43 | 4.27 | 0.00 | 45.54 | 45.54 | 24.19 | 7.71 |
| 11 | Plains | 0.41 | 34.06 | 33.66 | 20.01 | 5.88 | 0.00 | 26.74 | 27.70 | 11.36 | 6.52 | 0.00 | 23.70 | 24.75 | 5.92 | 6.37 | 0.00 | 7.80 | 8.15 | 1.56 | 2.25 | 0.00 | 33.41 | 33.41 | 18.96 | 5.80 |
| 12 | Plains | 0.58 | 39.96 | 39.38 | 25.31 | 6.61 | 0.00 | 36.18 | 36.70 | 15.63 | 7.04 | 0.00 | 31.14 | 31.97 | 8.76 | 7.30 | 0.00 | 22.26 | 22.71 | 2.99 | 5.02 | 0.76 | 39.55 | 38.79 | 23.67 | 6.38 |
| 13 | Plains | 0.47 | 36.40 | 35.93 | 23.01 | 6.12 | 0.00 | 31.10 | 32.29 | 13.42 | 7.74 | 0.00 | 27.09 | 27.62 | 7.30 | 7.03 | 0.00 | 6.45 | 6.60 | 1.26 | 2.35 | 1.02 | 35.50 | 34.48 | 21.74 | 6.09 |
| 14 | Plains | 0.39 | 40.96 | 40.57 | 22.57 | 9.06 | 0.00 | 36.60 | 37.04 | 13.56 | 8.75 | 0.00 | 32.35 | 32.92 | 8.00 | 7.74 | 0.00 | 14.55 | 15.12 | 3.08 | 4.83 | 0.00 | 39.43 | 39.43 | 21.12 | 8.41 |
| 15 | Plains | 0.06 | 43.10 | 43.04 | 21.16 | 8.38 | 0.00 | 35.91 | 36.80 | 13.04 | 8.30 | 0.00 | 38.08 | 38.90 | 8.60 | 7.87 | 0.00 | 21.41 | 21.93 | 8.18 | 8.43 | 0.00 | 40.89 | 40.89 | 19.71 | 8.24 |
| 16 | Plains | 0.18 | 37.21 | 37.03 | 21.34 | 7.45 | 0.00 | 31.77 | 32.71 | 13.08 | 6.50 | 0.00 | 27.54 | 28.40 | 8.06 | 6.53 | 0.00 | 15.49 | 16.14 | 3.86 | 5.01 | 0.00 | 35.92 | 35.92 | 19.74 | 7.16 |
| 17 | Plains | 2.56 | 45.15 | 42.59 | 24.50 | 8.93 | 0.00 | 41.50 | 41.91 | 15.51 | 7.90 | 0.00 | 36.86 | 37.86 | 9.94 | 7.49 | 0.00 | 28.36 | 29.29 | 5.28 | 6.23 | 2.64 | 43.30 | 40.66 | 22.38 | 8.14 |
| 18 | Plains | 0.15 | 37.42 | 37.27 | 21.42 | 6.47 | 0.00 | 34.00 | 34.67 | 13.17 | 6.93 | 0.00 | 26.04 | 26.86 | 8.16 | 6.82 | 0.56 | 16.48 | 15.92 | 5.49 | 5.15 | 0.15 | 36.81 | 36.66 | 19.83 | 6.03 |
| 19 | Plains | 2.32 | 45.05 | 42.73 | 29.02 | 8.40 | 0.00 | 42.00 | 42.46 | 17.51 | 8.49 | 0.00 | 31.98 | 32.71 | 10.41 | 8.13 | 0.00 | 20.10 | 20.85 | 5.74 | 6.89 | 0.16 | 45.18 | 45.02 | 26.94 | 8.35 |
| 20 | Plains | 0.06 | 40.20 | 40.15 | 17.30 | 8.28 | 0.00 | 35.33 | 36.18 | 10.89 | 6.78 | 0.00 | 25.63 | 26.65 | 7.44 | 6.05 | 0.00 | 11.91 | 12.77 | 3.31 | 4.06 | 0.00 | 37.31 | 37.31 | 15.81 | 7.68 |
| 21 | Plateau | 6.45 | 50.28 | 43.83 | 30.98 | 7.69 | 0.00 | 40.62 | 41.01 | 21.11 | 7.78 | 0.00 | 44.10 | 45.23 | 15.90 | 9.09 | 0.00 | 32.78 | 34.33 | 11.18 | 9.19 | 4.16 | 44.14 | 39.98 | 27.83 | 7.08 |
| 22 | Plateau | 0.40 | 48.70 | 48.31 | 26.33 | 8.90 | 0.00 | 43.41 | 44.49 | 17.04 | 9.27 | 0.00 | 38.72 | 39.48 | 11.71 | 9.24 | 0.00 | 23.91 | 24.72 | 7.54 | 8.06 | 0.29 | 46.25 | 45.96 | 24.37 | 8.58 |
| 23 | Plateau | 0.00 | 48.25 | 48.25 | 13.73 | 9.57 | 0.00 | 41.58 | 42.64 | 7.72 | 7.14 | 0.00 | 38.86 | 39.79 | 4.83 | 5.77 | 0.00 | 21.41 | 21.75 | 3.15 | 5.15 | 0.00 | 45.11 | 45.11 | 12.22 | 8.96 |
| 24 | Plateau | 0.55 | 67.08 | 66.53 | 27.16 | 10.61 | 0.00 | 59.02 | 60.55 | 17.90 | 10.29 | 0.00 | 45.75 | 49.78 | 11.85 | 9.95 | 0.00 | 28.67 | 29.30 | 5.39 | 7.24 | 0.00 | 62.72 | 62.72 | 24.89 | 10.29 |
| 25 | Plateau | 0.34 | 58.74 | 58.40 | 39.89 | 8.83 | 0.00 | 48.31 | 49.58 | 25.24 | 10.26 | 0.00 | 46.27 | 48.68 | 16.81 | 11.07 | 0.00 | 32.38 | 32.61 | 9.85 | 10.20 | 0.00 | 56.97 | 56.97 | 36.23 | 8.49 |
| 26 | Plateau | 0.11 | 57.07 | 56.96 | 29.06 | 9.64 | 0.00 | 50.05 | 52.10 | 19.57 | 9.79 | 0.00 | 46.88 | 48.99 | 14.88 | 11.35 | 0.00 | 38.55 | 40.36 | 9.63 | 10.51 | 0.00 | 55.40 | 55.40 | 26.66 | 9.30 |
| 27 | Plateau | 2.16 | 44.32 | 42.16 | 25.59 | 6.53 | 0.00 | 38.17 | 39.33 | 17.53 | 8.01 | 0.00 | 35.37 | 36.46 | 9.39 | 8.52 | 0.15 | 13.03 | 12.88 | 2.69 | 3.73 | 2.80 | 42.24 | 39.44 | 24.42 | 6.18 |
| 28 | Plateau | 1.13 | 49.68 | 48.55 | 30.15 | 9.73 | 0.00 | 43.80 | 44.78 | 19.76 | 9.29 | 0.00 | 44.71 | 45.74 | 12.41 | 9.54 | 0.00 | 26.12 | 26.73 | 5.86 | 6.07 | 0.78 | 48.27 | 47.49 | 27.58 | 9.44 |
| 29 | Plateau | 2.21 | 49.30 | 47.09 | 31.97 | 9.83 | 0.00 | 44.38 | 45.25 | 20.32 | 10.75 | 0.00 | 40.80 | 42.09 | 11.65 | 9.80 | 0.00 | 23.01 | 23.26 | 8.22 | 8.42 | 1.60 | 48.40 | 46.80 | 29.52 | 9.74 |
| 30 | Plateau | 0.61 | 48.44 | 47.83 | 25.75 | 7.83 | 0.00 | 44.44 | 46.01 | 17.31 | 8.93 | 0.00 | 40.24 | 41.04 | 10.39 | 8.74 | 0.00 | 27.46 | 27.48 | 7.54 | 7.71 | 0.26 | 46.89 | 46.63 | 24.31 | 7.94 |

Appendix C. Plot comparison of CMF biomass estimates from Ecosphere and our study.

| Plot | Type | Aboveground Biomass (Mg ha$^{-1}$) Ecosphere | Aboveground Biomass (Mg ha$^{-1}$) Our study | Aboveground Biomass Difference (Mg ha$^{-1}$) |
|---|---|---|---|---|
| 4 | Plains | 155.8347 | 138.2268 | -17.60788 |
| 5 | Plains | 195.8609 | 356.9173 | 161.05639 |
| 6 | Plains | 363.7966 | 321.3243 | -42.47228 |
| 9 | Plains | 290.3188 | 245.0569 | -45.26192 |
| 10 | Plains | 360.2891 | 386.0866 | 25.79747 |
| 12 | Plains | 180.734 | 363.449 | 182.715 |
| 13 | Plains | 297.5821 | 287.3125 | -10.26955 |
| 15 | Plains | 147.0932 | 354.0432 | 206.95 |
| 16 | Plains | 415.2387 | 336.9401 | -78.29863 |
| 17 | Plains | 209.0639 | 309.0351 | 99.97117 |
| 18 | Plains | 348.1088 | 331.3627 | -16.74609 |
| 20 | Plains | 406.514 | 238.1732 | -168.34075 |
| 21 | Plateau | 461.8428 | 411.6529 | -50.18988 |
| 23 | Plateau | 120.9582 | 143.1611 | 22.20287 |
| 26 | Plateau | 224.7761 | 534.0952 | 309.31906 |
| 28 | Plateau | 406.2974 | 480.3996 | 74.10224 |
| 29 | Plateau | 406.2717 | 394.9079 | -11.36377 |
| 30 | Plateau | 556.3944 | 358.6898 | -197.70461 |

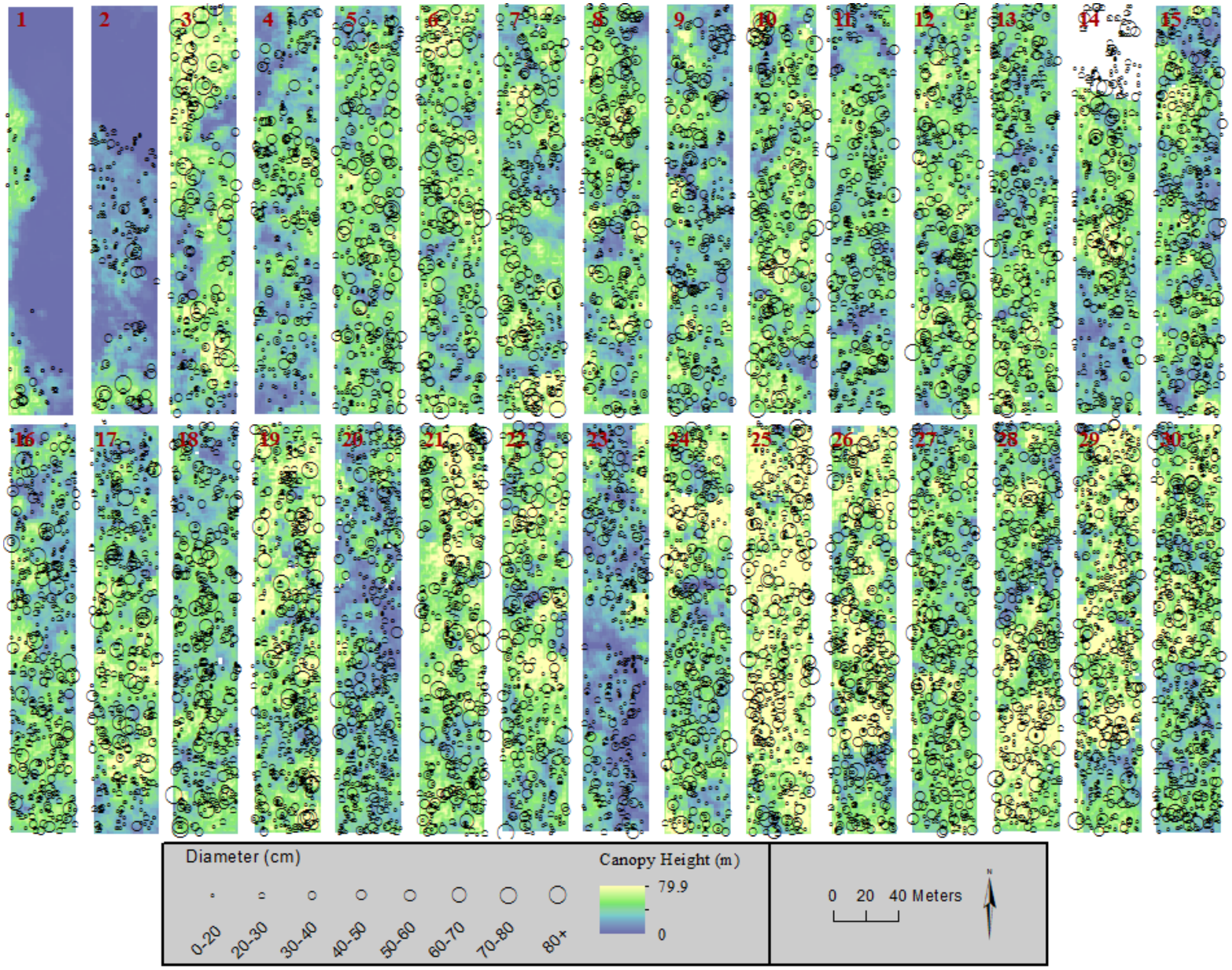


Appendix D. Stem maps for the 30 plots in ML2. Plots 1-20 are located in the plains forests, 21-30 are located in the plateau forests.

Appendix E. Photo of a skidder trail bisecting plot 23 and evidence of timber extraction.